

Executive Editor: FRANK A. PODOCK		Editorial Manager: LINDA TROWER Editorial Assistant: KAREN KLEIN KATY SMITH		Webmaster: ROBERT H. NEVREA, JR. Production Manager: CHRIS AUCHE	
ASSOCIATE EDITORS:	ROBERT C. ALPER JIMMY C. ALI YVES ANSELIN CAROL ANASTOI MELANIE BAR-MATHIEUX LINDA G. BRANDER THOMAS S. BRONNER JAY A. BRUNNER ALEX D. BRADSHAW DAVID J. BRIDGER ROBERT H. BRYAN WILLIAM H. CAGNEY THOMAS CHAPMAN JON CHAKOBER SARA COHEN DAVID R. COLE	CHRISTOPHER DAUGHNEY ZHENGGU DING JAMES FORTNEY FRIDRICH A. FRYX SCOTT GRADLER JOSHUA N. GOSWAMI JENNIFER R. HALL H. ROBERT HARVEY GREGORY R. HELL STUART R. HODSON GREGORY F. HODSON JIMMY HORTA TREVOR HURLAND JUN-ICHIRO ITOHASHI KAREN JOHANSSON CLARK JOHNSON	CHRISTIAN KERRIE RUSSELL KORTUM STEPHAN M. KRAEMER S. KUROSAWA ALEXANDER N. KRUT JAMES KURICKI GREGORY A. LAGAN TIMOTHY J. LYONS MICHAEL L. MACHENRY BERNARD MAREY TOM MCCALLUM ANDREW MERRIAM MARTIN A. MISHEN JACK J. MUEHLBERG ALONZO MUCCI BRIAN MYERS	HIROO NAGASAKA MARTIN NIKOLIC PIETRO A. OTTAVI FRANZ H. OBERGROSS DIMITRI PAPANASTASIADIS SANDRA PIZZARELLO MARK REICHBERGER W. URS REISCHLE EDWARD M. RIPLEY KAYON RORER J. KYLE RUSSELL SARA S. RUSSELL F. J. SVERDRUP JACQUES SUDREY JUDITH SWENOLD THOMAS J. SNOOK	J. S. SENSIGHER-DAMITE DONALD L. STUBBS DIMITRI A. SVETKEY MICHAEL J. TONIN PETER UHLEN DAVID J. VAUGHAN REINHARD J. WALKER LESLAY A. WARRIOR JOHN WARD ROD A. WOODHEAD CHEN ZHU
Volume 73, Number 3		February 1, 2009			
Articles					
M. BAUER, C. BLODAN: Arsenic distribution in the dissolved, colloidal and particulate size fraction of experimental solutions rich in dissolved organic matter and ferric iron					529
S. SERRANO, P. A. O'DAY, D. VLASSOPOULOS, M. T. GARCIA-GONZALEZ, F. GARRIDO: A surface complexation and ion exchange model of Pb and Cd competitive sorption on natural soils					543
J. D. WEBSTER, C. M. TAPPIN, C. W. MANDEVILLE: Partitioning behavior of chlorine and fluorine in the system apatite-melt-fluid. II: Felsic silicate systems at 200 MPa					559
N. KAUR, B. SINGH, B. J. KENNEDY, M. GRAPE: The preparation and characterization of vanadium-substituted goethite: The importance of temperature					582
H. C. HELGASON, L. RICHARD, W. F. MCKENZIE, D. L. NORTON, A. SCHMITT: A chemical and thermodynamic model of oil generation in hydrocarbon source rocks					594
J. MIOT, K. BENZERARA, G. MORIN, A. KAPPLER, S. BERNARD, M. OBST, C. FERARD, F. SGOURI-PANET, J.-M. GURONER, N. POSTH, M. GALVEZ, G. E. BROWN JR., F. GOYOT: Iron biomineralization by anaerobic neutrophilic iron-oxidizing bacteria					696
C.-Y. WANG, I. H. CAMPBELL, C. M. ALLEN, I. S. WILLIAMS, S. M. EGGINS: Rate of growth of the preserved North American continental crust: Evidence from Hf and O isotopes in Mississippi detrital zircons					712
F. HUANG, C. C. LUNDSTROM, J. GLESSNER, A. IANNO, A. BOUDREAU, J. LI, E. C. FERRÉ, S. MARSHAK, J. DEFRAITES: Chemical and isotopic fractionation of wet andesite in a temperature gradient: Experiments and models suggesting a new mechanism of magma differentiation					729
M. BLENBERG, R. SEFFERT, S. KASTEN, E. BAHLMANN, W. MICHAELIS: Epiflotic zone bacterioplankton sources major sedimentary bacteriopenepolyols in the Holocene Black Sea					750
H. LEROUX, M. ROKOSZ, D. JACOB: Oxidation state of iron and extensive redistribution of sulfur in thermally modified Stardust particles					767
<i>Continued on outside back cover</i>					

This article appeared in a journal published by Elsevier. The attached copy is furnished to the author for internal non-commercial research and education use, including for instruction at the authors institution and sharing with colleagues.

Other uses, including reproduction and distribution, or selling or licensing copies, or posting to personal, institutional or third party websites are prohibited.

In most cases authors are permitted to post their version of the article (e.g. in Word or Tex form) to their personal website or institutional repository. Authors requiring further information regarding Elsevier's archiving and manuscript policies are encouraged to visit:

<http://www.elsevier.com/copyright>



Thermodynamic constraints on hydrogen generation during serpentinization of ultramafic rocks

Thomas M. McCollom^{a,*}, Wolfgang Bach^b

^a *CU Center for Astrobiology and Laboratory for Atmospheric and Space Physics, Campus Box 392, University of Colorado, Boulder, CO 80309-0392, USA*

^b *Geoscience Department, University of Bremen, Klagenfurter Str., 28359 Bremen, Germany*

Received 12 December 2007; accepted in revised form 21 October 2008; available online 8 November 2008

Abstract

In recent years, serpentinized ultramafic rocks have received considerable attention as a source of H₂ for hydrogen-based microbial communities and as a potential environment for the abiotic synthesis of methane and other hydrocarbons within the Earth's crust. Both of these processes rely on the development of strongly reducing conditions and the generation of H₂ during serpentinization, which principally results from reaction of water with ferrous iron-rich minerals contained in ultramafic rocks. In this report, numerical models are used to investigate the potential influence of chemical thermodynamics on H₂ production during serpentinization. The results suggest that thermodynamic constraints on mineral stability and on the distribution of Fe among mineral alteration products as a function of temperature are likely to be major factors controlling the extent of H₂ production. At high temperatures (>~315 °C), rates of serpentinization reactions are fast, but H₂ concentrations may be limited by the attainment of stable thermodynamic equilibrium between olivine and the aqueous fluid. Conversely, at temperatures below ~150 °C, H₂ generation is severely limited both by slow reaction kinetics and partitioning of Fe(II) into brucite. At 35 MPa, peak temperatures for H₂ production occur at 200–315 °C, indicating that the most strongly reducing conditions will be attained during alteration within this temperature range. Fluids interacting with peridotite in this temperature range are likely to be the most productive sources of H₂ for biology, and should also produce the most favorable environments for abiotic organic synthesis. The results also suggest that thermodynamic constraints on Fe distribution among mineral alteration products have significant implications for the timing of magnetization of the ocean crust, and for the occurrence of native metal alloys and other trace minerals during serpentinization.

© 2008 Elsevier Ltd. All rights reserved.

1. INTRODUCTION

Fluids discharged from serpentinites have frequently been observed to be highly enriched in H₂ and CH₄ (Barnes and O'Neil, 1969; Neal and Stanger, 1983; Abrajano et al., 1988, 1990; Charlou and Donval, 1993; Charlou et al., 1998, 2002; Kelley and Früh-Green, 1999; Kelley et al., 2001, 2005; Takai et al., 2004). In recent years, there has been an increasing interest in the potential for the H₂ and CH₄ in these fluids to support communities of chemolithoautotrophic microorganisms in surface and subsurface environments in

both continental and seafloor settings (e.g., Alt and Shanks, 1998; Kelley et al., 2001, 2005; Takai et al., 2004; Nealson et al., 2005; Alt et al., 2007; McCollom, 2007). Fed by metabolic energy sources including hydrogen oxidation, methanogenesis, and methanotrophy, these microbial communities can exist with little or no input from photosynthesis, and could thus represent analogs for life on the early Earth or other planetary bodies (Fisk and Giovannoni, 1999; McCollom, 1999; Chapelle et al., 2002; Takai et al., 2004, 2006; Schulte et al., 2006). In addition, high abundances of methane as well as other hydrocarbons in serpentinite-derived fluids have led to suggestions that abiotic synthesis of organic compounds occur in these environments through reduction of CO₂ or CO by H₂ (Berndt et al., 1996; Holm and Andersson, 1998; Shock and Schulte, 1998; Horita and Berndt, 1999; Holm

* Corresponding author.

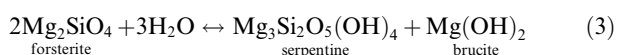
E-mail addresses: mccollom@lasp.colorado.edu (T.M. McCollom), wbach@uni-bremen.de (W. Bach).

The occurrence of Fe in serpentine and brucite suggests that the generation of H₂ may be significantly diminished by partitioning of Fe(II) into product minerals, particularly during serpentinization where large amounts of Fe-rich brucite precipitate. At the present time, however, there appears to be little understanding of the factors that regulate how much Fe(II) is partitioned into alteration minerals during serpentinization. Consequently, it remains unclear how Fe(II) partitioning affects the amounts and rates of H₂ generation, and how the partitioning is controlled by variables such as temperature, reactant rock and fluid composition, water:rock ratio, etc.

A critical property of ultramafic rocks that allows abundant H₂ production to occur during serpentinization is that the low silica activity of the rocks (Frost and Beard, 2007) results in formation of alteration minerals (particularly serpentines and brucite) that tend to largely exclude Fe(II) from their structure, leading to formation of magnetite (and, consequently, H₂). In more silica-rich rocks such as basalts, a greater proportion of Fe(II) is sequestered in silicate alteration minerals such as chlorite and amphibole which more readily allow Fe(II) into their structure, rather than being converted to Fe(III). As a result, hydrothermal alteration of basalt generates much lower amounts of H₂ than serpentinization of ultramafic rocks, even though the Fe(II) content of basalt is typically much higher. For example, deep-sea hydrothermal fluids interacting with hot basalt typically have H₂ concentrations in the 0.05–1.7 mmol kg⁻¹ range (Von Damm, 1995), while H₂ concentrations of 12–16 mmol kg⁻¹ are reported for submarine hydrothermal fluids that have interacted with ultramafic rocks (Charlou et al., 2002; Kelley et al., 2005). Even higher H₂ concentrations exceeding 100 mmol kg⁻¹ are indicated by the presence of native metal alloys in many serpentinites (Frost, 1985; Alt and Shanks, 2003) and have been produced in experimental studies of serpentinization (Berndt et al., 1996; McCollom and Seewald, 2001). Thus, serpentinites appear to be unique in their capacity to generate high H₂ abundances.

3. THERMODYNAMIC CONSTRAINTS ON H₂ GENERATION

Thermodynamic considerations have been employed for several decades to place constraints on physical conditions during serpentinization (see, for instance, Evans and Trommsdorf, 1972; O'Hanley, 1996; Mével, 2003; Früh-Green et al., 2004). In most cases, these studies have taken the approach of using univariant curves for individual phase equilibria in order to evaluate pressure and temperature conditions during serpentinization based on petrologic observations. For example, Fig. 1 shows univariant curves for equilibrium of the reactions:



and

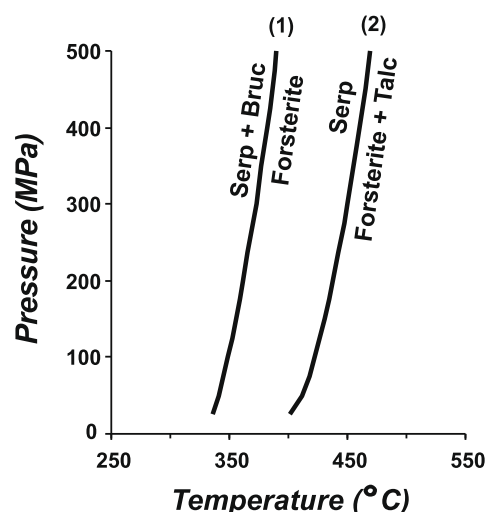
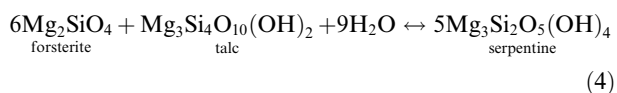


Fig. 1. Univariant curves for the reactions (1) forsterite + H₂O = serpentine + brucite and (2) forsterite + talc + H₂O = serpentine.

Comparison of the boundaries imposed by equilibria such as these with mineral assemblages observed in a particular rock sample allows constraints to be placed on the conditions that were present during crystallization. But, few studies using this approach have considered the impact of mineral solid solution compositions on equilibrium, or their effect on fluid composition. Recently, however, Sleep et al. (2004) used a phase equilibria approach to evaluate H₂ concentrations in equilibrium with varying solid solution compositions for serpentine, brucite, and Ni,Fe-alloys (e.g., awaruite).

The phase equilibria approach is useful for interpreting alteration conditions for rocks whose mineral composition is known (for example, by examination of thin sections). However, this method has little predictive value and provides little information on fluid composition (except, perhaps, for evaluating the activity of CO₂ in carbonate-bearing assemblages). For instance, while a phase equilibria approach can be used to determine H₂ concentrations in equilibrium with mineral solid solutions of a given composition (e.g., Sleep et al., 2004), it is not possible to use this approach to predict what mineral compositions would be attained during alteration of a particular ultramafic rock, or to estimate the amount of H₂ that would be generated during that alteration. Furthermore, the phase equilibria approach provides no insight into how or why the rock arrived at a particular mineral composition, nor does it allow a means of assessing the impact of the original rock and fluid composition on alteration mineralogy.

For this study, thermodynamic constraints on fluid and mineral composition during serpentinization were explored through the use of reaction path models. These models emulate reactions of minerals with a fluid, and determine the compositions of minerals and coexisting fluid that would be attained at thermodynamic equilibrium for a given temperature and pressure by minimizing the Gibbs energy of the overall system. By taking into account mass balance and variable solid solution compositions during

reaction, these models allow investigation of additional constraints on mineral and fluid compositions during serpentinization that cannot be evaluated using a phase equilibria approach. Several previous studies have employed reaction path models to examine various aspects of serpentinization (Wetzel and Shock, 2000; Alt and Shanks, 2003; Allen and Seyfried, 2003; Palandri and Reed, 2004). However, these previous studies considered a limited range of temperatures and solid solution compositions, and do not address variables involved in H_2 production. The models presented here expand beyond these previous efforts by considering a larger range of conditions (temperature, water:rock ratio), incorporate solid solutions for serpentine, brucite, and other minerals, and focus on factors effecting the generation of H_2 .

The models performed for this study primarily examine the affects of temperature and water:rock ratio on mineral and fluid compositions during fluid–rock interactions. The calculations require definition of the composition of the initial rock and fluid as inputs for the models. Because it is most representative of ultramafic rocks exposed to fluid circulation beneath the seafloor, the calculations presented here are performed for rocks with a harzburgitic composition. Accordingly, the reactant rock was composed of 80 wt% olivine (Mg# = 0.90; equivalent to 5.419 moles $Mg_{1.8}Fe_{0.2}SiO_4$ per kg of rock), 15 wt% orthopyroxene (Mg# = 0.85; 1.427 moles $Mg_{0.85}Fe_{0.15}SiO_3$ kg^{-1}), and 5 wt% clinopyroxene (Mg# = 0.90; 0.228 moles $CaMg_{0.9}Fe_{0.1}Si_2O_6$ kg^{-1}). The initial fluid reactant was presumed to be composed of seawater depleted in O_2 and sulfate, with Ca and Mg partially removed to achieve charge balance (Table 1). This fluid is nominally intended to represent seawater whose composition has been modified by circulation through the crust.

All calculations shown here are performed for a pressure of 35 MPa, appropriate to shallow subseafloor environments or intermediate depths within the continental crust. It should be borne in mind that the calculations are most relevant to reaction at this pressure, and the temperature ranges discussed for phase relationships will vary somewhat for serpentinization at other pressures. In general, the temperatures of phase transitions in this system increase with increasing pressure (Fig. 1). However, the relative thermo-

Table 1
Initial fluid composition used in the models.

Component	Concentration
pH	7.8
Na^+	464.
Cl^-	546.
HCO_3^-	2.3
Ca^{2+}	10.2
Mg^{2+}	24.8
K^+	9.8
$SiO_{2(aq)}$	0.16
Fe	0.0000015
SO_4^{2-}	0
$O_{2(aq)}$	0

All concentrations in mmolal.

Table 2
List of solid solutions included in the thermodynamic database.

Solid solution	Components
Orthopyroxene	Enstatite
	Ferrosilite
Clinopyroxene	Diopside
	Hedenbergite
Serpentine	Chrysotile
	Greenalite
Brucite	Brucite
	$Fe(OH)_2$
Talc	Talc
	Minnesotaite
Amphibole	Tremolite
	Ferrotremolite

dynamic properties of the phases involved in serpentinization reactions are relatively insensitive to pressure, so that moderate increases in pressure (up to a few 100 MPa) results in an increase of only a few tens of degrees for the reactions under study.

The model calculations were performed using the computer program EQ3/6, version 7.2b (Wolery, 1992; Wolery and Daveler, 1992), with a customized thermodynamic database² for 35 MPa compiled using SUPCRT92 (Johnson et al., 1992). The computations included all minerals and inorganic aqueous species in the SUPCRT92 database for the system Mg-Ca-Fe-Si-Na-Cl-O-H, except as noted below. SUPCRT92 incorporates thermodynamic data from Helgeson et al. (1978) for minerals, and Shock and Helgeson (1988) and Shock et al. (1989, 1997) for dissolved inorganic aqueous species. Activity coefficients for aqueous species are calculated using the B-dot equation (Helgeson et al., 1981).

Although alteration of ultramafic rocks generates several different serpentine minerals including lizardite, antigorite, and chrysotile (e.g., Moody, 1976a; O'Hanley, 1996; Mével, 2003; Früh-Green et al., 2004), chrysotile was used in the models to represent the serpentine group. In large part, this restriction is based on the lack of thermodynamic data for the other phases, since the Helgeson et al. (1978) mineral database does not include lizardite and thermodynamic data for the Fe-end member corresponding to antigorite are not available. However, because the differences in thermodynamic properties among the different serpentine minerals are likely to be very small relative to the differences between the serpentines and other minerals in the database, this assumption is likely to have a relatively minor impact on the outcome of the models. Solid solutions are included in the models for many minerals, as listed in Table 2. Owing to a lack of reliable data for the thermodynamic properties of mixing for these solid solutions, ideal site mixing was assumed for all solid solutions. Only Fe-for-Mg exchange is considered for these solid solutions.

² Electronic copies of the database and EQ3/6 input files are available from the authors on request.

In some cases, thermodynamic parameters for minerals and solid solutions that are particularly relevant to the study of serpentinites were not available in the SUPCRT92 database and had to be estimated or incorporated from other sources. Specifically, the database lacks data for the standard Gibbs energy of formation (ΔG°_f) for greenalite, minnesotaite, and $\text{Fe}(\text{OH})_2$ (Fe-endmembers of chrysotile, talc, and brucite solid solutions, respectively), and standard entropy (S°) and heat capacity (ΔC_p) data for $\text{Fe}(\text{OH})_2$. For this study, $\Delta G^\circ_{f,\text{greenalite}}$ was adopted from Sassani (1992), $\Delta G^\circ_{f,\text{minnesotaite}}$ was taken from Sverjensky (1992), and $\Delta G^\circ_{f,\text{Fe}(\text{OH})_2}$ from Sverjensky and Molling (1992). Heat capacity (C_p) as a function of temperature for $\text{Fe}(\text{OH})_2$ was estimated from that of brucite by assuming that the impact of Mg-for-Fe substitution on heat capacity between brucite and $\text{Fe}(\text{OH})_2$ is the same as that for chrysotile and greenalite. That is, heat capacities for $\text{Fe}(\text{OH})_2$ are calculated according to the equation:

$$C_{p,\text{Fe}(\text{OH})_2} = C_{p,\text{brucite}} + 0.33(C_{p,\text{greenalite}} - C_{p,\text{chrysotile}}) \quad (5)$$

where the factor of 0.33 accounts for the presence of three Mg per formula unit for chrysotile. Chrysotile is composed of alternating layers of silica tetrahedra and $\text{Mg}(\text{OH})_2$ (often referred to as the “brucite layer”), and the greenalite structure involves substitution of Fe for Mg in the $\text{Mg}(\text{OH})_2$ layer. Because the site of this substitution is structurally similar to the site of Mg in the $\text{Mg}(\text{OH})_2$ layers that compose brucite, this appears to be the most reasonable approach to estimating the thermodynamic properties of $\text{Fe}(\text{OH})_2$. Values of C_p as a function of temperature were calculated using Maier–Kelley power function coefficients from Helgeson et al. (1978) as included in the SUPCRT92 database (Johnson et al., 1992). The standard entropy for $\text{Fe}(\text{OH})_2$ ($=88 \text{ J mol}^{-1} \text{ K}^{-1}$) was taken from Wagman et al. (1982) and the molar volume ($=30.5 \text{ cm}^3 \text{ mol}^{-1}$) is from Kozlov and Levshov (1962). The thermodynamic parameters adopted for these minerals are summarized in Table 3.

As described below, olivine can be thermodynamically stable during fluid–rock interactions with ultramafic rocks at high temperature ($>\sim 315^\circ \text{C}$ at 35 MPa). During the initial calculations for this study, the composition of olivine solid solution during alteration was allowed to vary freely, and it was observed that the composition of the olivine at equilibrium would become slightly more enriched in Mg than the starting material (i.e., olivine with an initial $\text{Mg}\# = 0.90$ would alter to $\text{Mg}\# = 92\text{--}94$

during equilibration with the fluid at high temperatures for the rock composition employed in the model). However, this did not appear to be geologically realistic, since partially altered olivine in serpentinites do not generally show a significant change in composition that would correspond to the Fe-for-Mg exchange predicted by the equilibrium models. Therefore, the composition of olivine was fixed in the models at $\text{Mg}\# = 0.90$ in all calculations, so that olivine retains its original composition throughout the calculation. The compositions of all other solid solutions were allowed to vary freely over their entire range.

Owing to a lack of thermodynamic data, the database employed in the models excludes a number of accessory minerals that are commonly used to interpret the oxidation state of the system during serpentinization, including native metal alloys and Ni-bearing sulfides (e.g., Frost, 1985; Alt and Shanks, 1998). However, the low abundance of these minerals indicates that they are unlikely to be the primary components controlling the abundance of H_2 during serpentinization, but, rather, are responding to the oxidation state controlled by the more abundant silicates, magnetite, and brucite. Consequently, omission of these minerals probably has only a small effect on estimates of H_2 generation in the models. Extension of the database and models to include these minerals will be an objective of a follow-up study.

Reaction path models such as these have inherent uncertainties arising from both the numerical methods employed in the calculations and the underlying thermodynamic database. However, because of the many assumptions and extrapolations that are required in order to derive the requisite thermodynamic parameters (including, but not limited to, those mentioned above), quantitative assessment of these uncertainties is problematic (see, for example, discussion in Helgeson et al., 1978). Stated uncertainties in standard Gibbs energies for individual aqueous species are on the order of $\sim 0.1 \text{ kJ mol}^{-1}$ at standard state conditions of 25°C and 0.1 MPa, but these uncertainties increase significantly at elevated temperatures and pressures (Shock and Helgeson, 1988). At 300°C and 35 MPa, uncertainties are apparently on the order of $1.5\text{--}2 \text{ kJ mol}^{-1}$. Individual minerals have apparent uncertainties of a similar magnitude (Helgeson et al., 1978). How these errors in thermodynamic data for individual compounds propagate into numerical models that include numerous minerals and aqueous species is unclear. The assumption of ideality for solid solutions and estimates of the thermodynamic properties for some endmembers adds an additional level of uncertainty to the calculations, but the current lack of experimental data concerning phase relations in these systems precludes quantitative evaluation of the accuracy of the resulting predictions. Below, however, we do consider the impact of the estimated thermodynamic properties of $\text{Fe}(\text{OH})_2$ on the outcome of the models. Owing to these limitations, the model results presented here should be regarded as provisional predictions until more definitive thermodynamic data become available from laboratory experiments, and models results should be considered as approximations rather than precise values.

Table 3

Thermodynamic data for Fe endmembers of solid solutions adopted in the geochemical models, including standard Gibbs energy of formation (ΔG°_f), standard entropy (S°), and Maier–Kelley coefficients (a , b , and c) used in calculations of the heat capacity (C_p) by SUPCRT92 (see Johnson et al., 1992).

Mineral	ΔG°_f (kJ mol^{-1})	S° ($\text{J mol}^{-1} \text{ K}^{-1}$)	a	b ($\times 10^3$)	c ($\times 10^{-5}$)
$\text{Fe}(\text{OH})_2$	−492.82	88.00	109.06	18.192	−22.52
Minnesotaite	−4392.79	349.53	369.67	178.37	−46.67
Greenalite	−2994.41	303.90	341.79	136.46	−64.42

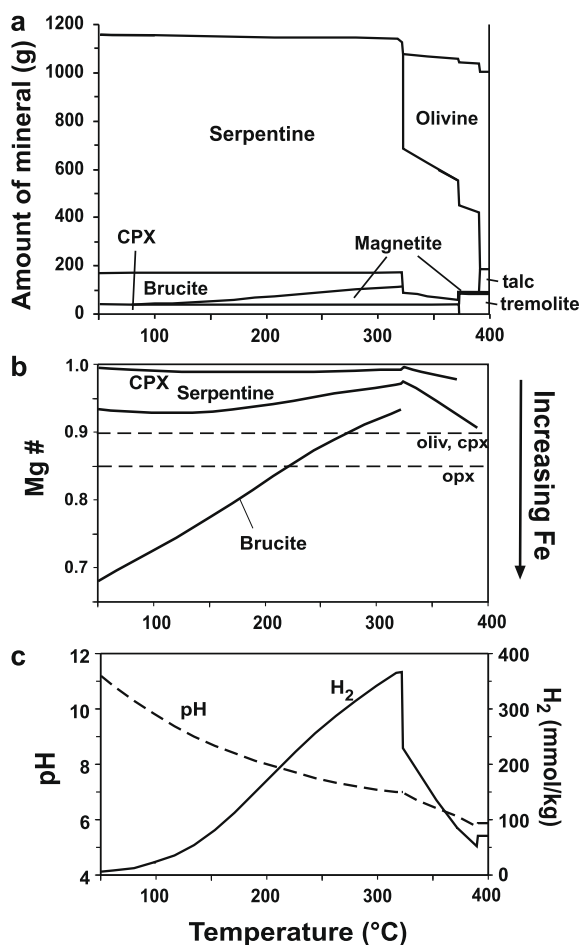


Fig. 2. Predicted alteration mineralogy and fluid composition during hydrothermal alteration of harzburgite for a range of temperatures at a water:rock ratio equal to one. (a) Equilibrium mineral composition in amount of mineral per kilogram harzburgite reacted. (b) Mineral solid solution compositions. (c) Fluid pH and H₂ concentration. Dashed lines in (b) indicate composition of mineral solid solutions in the original harzburgite. Abbreviations: “oliv” = olivine, “opx” = orthopyroxene, “cpx” = clinopyroxene.

3.1. Temperature dependence

We first use the thermodynamic models to examine the effect of temperature on rock and fluid composition during serpentinization. Fig. 2 shows model results for the reaction of harzburgite with seawater over a range of temperatures from 50 °C to 400 °C and a constant water:rock ratio of 1. Fig. 2a shows the predicted equilibrium mineral assemblage as a function of temperature. At all temperatures below 315 °C, the equilibrium mineral assemblage consists of a typical serpentinite composition that includes serpentine, brucite, magnetite, and minor secondary clinopyroxene (diopside), with serpentine the predominant mineral. Above 315 °C, olivine becomes a stable member of the assemblage, and will coexist in equilibrium with the fluid and alteration minerals after it has only partially reacted. The inclusion of olivine eliminates brucite from the equilibrium assemblage. The proportion of unaltered olivine among the equilibrium

minerals increases with temperature from 315 °C up to 390 °C, and above this temperature the amount of unaltered olivine present at equilibrium is essentially identical to that in the original rock (a very small amount of olivine dissolves to bring the mineral into equilibrium with the fluid above 390 °C). At temperatures between 370 °C and 390 °C, the equilibrium assemblage consists of serpentine, tremolite and a small amount of magnetite produced from alteration of pyroxenes, along with relict unreacted olivine (the amount of magnetite produced, 10–18 g per kg harzburgite, is too small to be readily apparent in Fig. 2a). Above 390 °C, talc replaces serpentine as an alteration mineral, so that the equilibrium assemblage consists of unaltered olivine along with talc, tremolite, and a small amount of magnetite produced from decomposition of pyroxenes.

The results in Fig. 2a show that partially reacted olivine can stably coexist with alteration minerals over a broad temperature range. Whereas the univariant approach would indicate that olivine and serpentinite should be stable together only at a single temperature for a given pressure (Fig. 1), when mass balance constraints are taken into account the transition between olivine and serpentinite occurs over a range of temperatures (315–390 °C for the modeled conditions). Within this temperature range, olivine will react only until it reaches equilibrium with the encroaching fluid and the other minerals in the alteration assemblage, and then will cease to react further. Above 390 °C, only a very small amount of olivine reaction is required to reach equilibrium, so that olivine remains almost completely unaltered. Typically, incompletely serpentinized rocks with unaltered olivine are interpreted as reflecting either insufficient time or too little water to allow the reaction to go to completion. However, the results shown in Fig. 2a suggest that some partially serpentinized rocks could reflect an equilibrium condition at temperatures above ~315 °C. At these temperatures, partially serpentinized olivine can persist stably for indefinite periods of time, and in the presence of excess water.

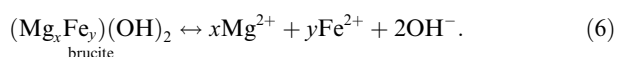
Solid solution compositions corresponding to the equilibrium mineral assemblages portrayed in Fig. 2a are shown in Fig. 2b. At all temperatures, the proportion of Fe predicted by the models to be incorporated into serpentine is less than that of the initial reactant minerals (i.e., Mg# > 0.9 for serpentine versus Mg# = 0.9 for olivine and clinopyroxene and Mg# = 0.85 for orthopyroxene). Brucite, on the other hand, is depleted in Fe relative to the primary minerals at high temperatures, but incorporates an increasing amount of Fe(II) with decreasing temperature, so that at lower temperatures the Fe-endmember of brucite constitutes a substantial fraction of the mineral solid solution. At temperatures below ~200 °C, the proportion of Fe incorporated into brucite exceeds that of the primary olivine and orthopyroxene (i.e., Mg# < 0.85). Because a greater amount of the Fe from the primary minerals is incorporated into brucite, the amount of Fe converted to magnetite decreases with decreasing temperature (Fig. 2a). Secondary clinopyroxene in the equilibrium alteration assemblage is essentially pure diopside at all temperatures (Mg# ≈ 0.98), suggesting that recrystallization of

clinopyroxene should occur during lower temperature alteration (<~315 °C) that results in loss of Fe. Talc and tremolite predicted to form at >370 °C are essentially pure Mg end-members (Mg# > 0.98).

The pH and H₂ concentration of the fluid in equilibrium with the minerals is shown in Fig. 2c. It can be seen from this figure that the predicted concentration of H₂ at equilibrium varies strongly with temperature, attaining a peak of ~360 mmolal at 315 °C and decreasing sharply at both higher and lower temperatures, reaching <70 mmolal at 400 °C and only ~7 mmolal at 50 °C. Since production of H₂ during serpentinization occurs largely as a consequence of the formation of magnetite (Rxn. 2), the reduction in concentration of H₂ at lower temperatures reflects the increased partitioning of Fe(II) into brucite and decrease in magnetite formation with decreasing temperature (Fig. 2a and b). At temperatures around 150 °C, the amount of H₂ generated at equilibrium for a water:rock ratio of one is predicted to be <25% of that occurring from the same amount of rock alteration at higher temperatures near 300 °C, dropping to less than 3% at 50 °C.

The production of H₂ also decreases at temperatures above 315 °C, but in this case the amount of H₂ generated is limited by attainment of thermodynamic equilibrium between olivine, the fluid, and secondary alteration minerals. At these temperatures, alteration ceases when the original olivine is only partially reacted, decreasing the amount of Fe converted to magnetite. The extent of olivine reacted and, consequently, the amount of magnetite formed decreases with increasing temperature above 315 °C. Although it is difficult to discern in Fig. 2a, a small amount of magnetite is still produced above the temperature where olivine becomes essentially unreactive (>~370 °C) owing to reaction of pyroxenes. As a consequence of pyroxene reaction, substantial concentrations of H₂ are still generated at equilibrium (50–80 mmolal) even without the involvement of olivine, albeit at levels significantly less than those attained at lower temperatures where olivine is reactive.

The equilibrium pH is near neutrality at high temperatures, but becomes increasingly alkaline at lower reaction temperatures, reaching a pH of ~11 at 50 °C (Fig. 2c). The pH is largely determined by equilibrium of the fluid with brucite, which can be represented by the general reaction:



The equilibrium constant for this reaction increases with decreasing temperature, favoring higher dissolved concentrations of OH⁻. However, the pH is dependent not only on the equilibrium constant for this reaction but also on the levels of dissolved Mg and Fe, which are regulated in turn by equilibrium with the other minerals present in the alteration assemblage. Thus, the pH is ultimately controlled by the entire mineral assemblage and not just brucite.

Concentrations of dissolved elements in equilibrium with the mineral assemblages shown in Fig. 2 are given in Fig. 3, where it can be seen that variations in the fluid composition as a function of temperature are relatively minor (note that concentrations in Fig. 3 are represented on a log scale so that

all elements can be displayed, and this scale exaggerates minor variations in elements present at low abundance). Except at high temperature, the fluid is enriched in Ca, slightly depleted in Si, and strongly depleted in Mg relative to the starting solution. Dissolved concentrations of Si, Mg, and Fe are predicted to increase substantially during reaction at higher temperatures, increasing by more than two orders of magnitude between 315 °C and 400 °C. However, even at the highest temperatures the concentrations of these elements remain below a couple of mmolal.

3.2. Dependence on water:rock ratio

The impact of water:rock ratio (W:R) on alteration mineralogy and fluid composition during serpentinization varies significantly as a function of temperature. This can be illustrated by examining the effect of varying water:rock ratio on thermodynamic equilibrium at three representative temperatures, with 100 °C representing the low temperature range (50 °C to ~200 °C), 300 °C the intermediate temperature range where H₂ generation is highest (~200 °C to 315 °C), and 350 °C representing the range where olivine persists in equilibrium with secondary alteration products after only partial reaction (315–390 °C). These temperatures are considered individually in the following subsections.

At all temperatures, reaction at low W:R results in a large fraction of the water being incorporated into hydrated alteration minerals at equilibrium, leading to steeply increased salinity and concentrations of dissolved compounds in the remaining fluid. The thermodynamic data on which the models are based are only appropriate for total dissolved solute concentrations up to ~2–3 molal (Wolery, 1992). Owing to the concentration of solutes by incorporation of water into hydrated minerals, this limit is exceeded at low water:rock ratios in the equilibrium calculations. Consequently, model results for W:R < ~0.2 were considered to be too unreliable to include in the discussion, and results for W:R < ~0.3 should probably be considered as provisional. In all cases, water:rock ratio in the following discussion refers to the value at the start of the reaction, not the relative amounts present at equilibrium.

3.2.1. Variation with water:rock ratio at 100 °C

Calculated equilibrium mineral assemblages and fluid compositions as a function of water:rock ratio at a constant temperature of 100 °C are shown in Fig. 4. Serpentine dominates the equilibrium mineral assemblage over the entire range of W:R studied, with lesser amounts of brucite, magnetite, and secondary clinopyroxene (diopside) (Fig. 4a). The fraction of magnetite in the mineral assemblages decreases substantially at lower water:rock ratio, while secondary diopside is not present in the equilibrium assemblage at W:R > ~6 because concentrations of Ca and Si remain below saturation levels for diopside at high ratios. The proportion of Fe in serpentine is lower than the initial harzburgite minerals at all water:rock ratios while that of brucite is higher than the starting minerals (Fig. 4c). For both minerals, the Fe content increases gradually with decreasing water:rock ratios.

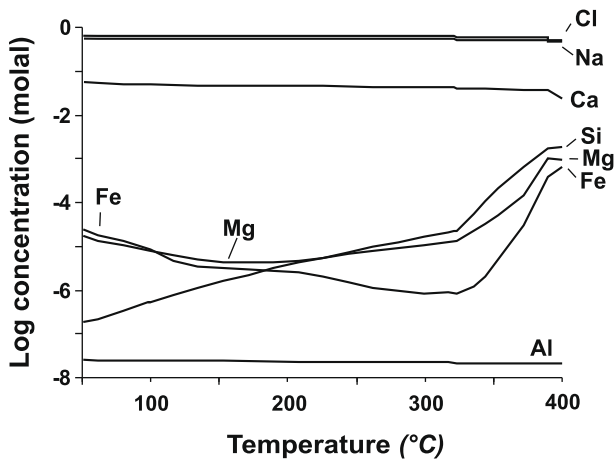


Fig. 3. Predicted total concentrations of dissolved elements in the fluid in equilibrium with the mineral assemblages shown in Fig. 2 for hydrothermal alteration of harzburgite as a function of temperature at a water:rock ratio of 1.

At lower water:rock ratios, an increasingly large fraction of the initial water is incorporated into hydrated minerals, so that only ~20% of the initial H₂O remains at equilibrium for W:R = 0.2 (Fig. 5b). Largely as a consequence of the

uptake of water into minerals, the concentrations of most dissolved elements increase steadily with decreasing water:rock ratio (Fig. 4d). However, the relative levels of dissolved elements are also somewhat dependent on equilibrium with the mineral products. The pH remains essentially constant at ~9.7 except at very large W:R, reflecting buffering by the mineral assemblage (Fig. 4b). At water:rock ratios >~6, all Ca from the harzburgite is dissolved into the aqueous phase without reaching saturation with respect to diopside, allowing high concentrations of Mg and lower pH in the fluid.

The equilibrium concentration of dissolved H₂ is calculated to be around 15 mmolal at high W:R, and increases gradually with decreasing water:rock ratios to plateau at around 24 mmolal for W:R < 0.7 (Fig. 4b). These concentration levels are affected by several different factors. Although H₂ concentrations are higher at lower water:rock ratios, the amount of H₂ that is generated from each kilogram of harzburgite actually increases steeply with increasing water:rock ratios from 0.9 moles H₂ per kg of rock at W:R = 0.2 to ~130 moles kg⁻¹ at W:R = 10 (Fig. 5a). However, because the H₂ generated is dissolved into a larger amount of fluid at higher water:rock ratios, the resulting concentrations end up being lower. This effect is compounded at low water:rock ratios by incorporation of a larger fraction of H₂O from the initial fluid into hydrated

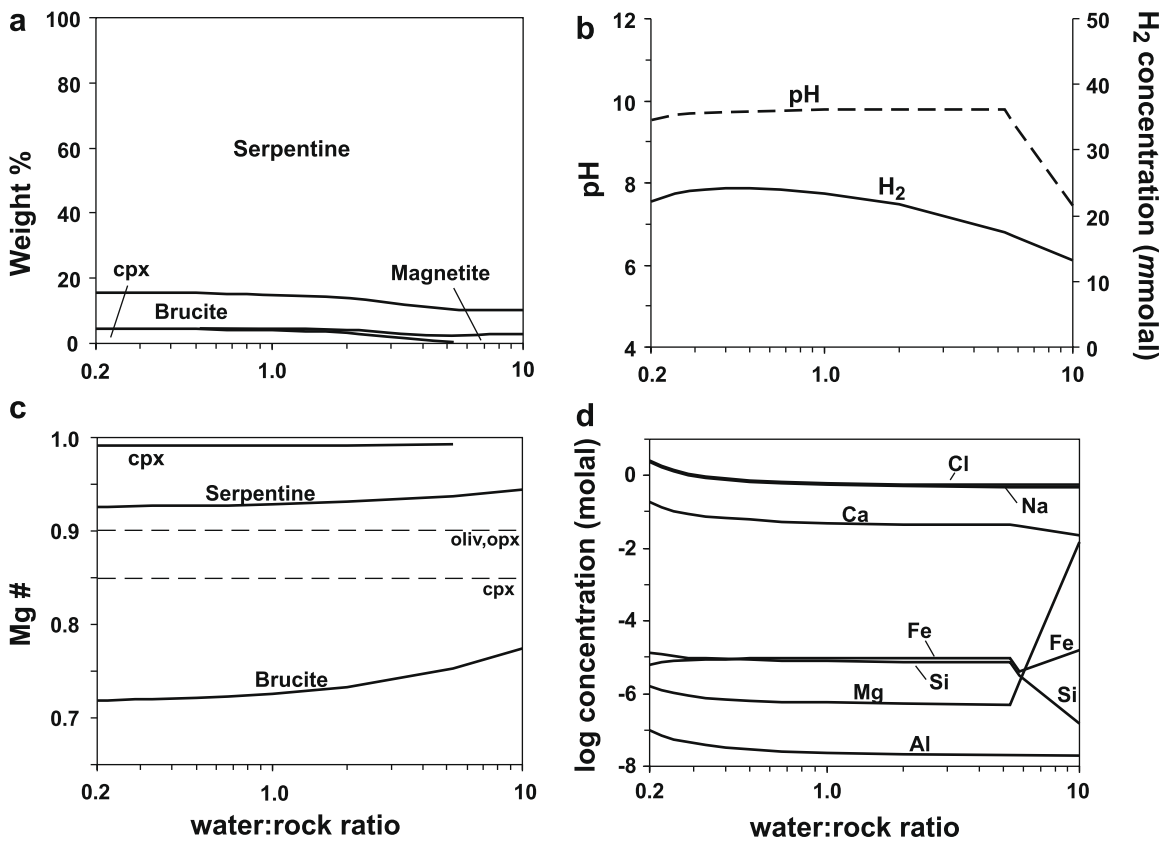
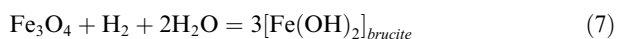


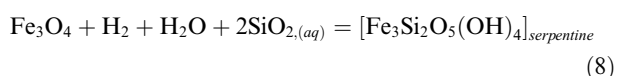
Fig. 4. Predicted equilibrium mineral and fluid compositions for hydrothermal alteration of harzburgite at 100 °C over a range of water:rock ratios. (a) Weight percent of minerals in the alteration assemblage, (b) pH and H₂ concentrations, (c) solid solution compositions, and (d) fluid composition. Dashed lines in (c) indicate composition of mineral solid solutions in the original harzburgite.

minerals (Fig. 5b), further concentrating the H₂ in the remaining fluid. The overall result is that H₂ concentrations decrease with increasing water:rock ratio even though more H₂ is being generated from each kg of rock, and concentrations are highest when the least amount of H₂ is generated per a given amount of rock.

Because the dissolved H₂ is maintained through equilibrium with the mineral phases, higher H₂ concentrations at lower water:rock ratios coincide with increased partitioning of Fe(II) into brucite and serpentine, and reduced production of magnetite (Fig. 4). These relationships can be portrayed by the generalized reactions:



and



where $[\text{Fe}(\text{OH})_2]_{\text{brucite}}$ and $[\text{Fe}_3\text{Si}_2\text{O}_5(\text{OH})_4]_{\text{serpentine}}$ represent Fe components of brucite and serpentine solid solutions. Higher H₂ concentrations require higher activities of the Fe components in brucite and serpentine in order to maintain equilibrium, shifting Fe from magnetite into these other minerals. Alternatively, one might look at these relationships from the point of view that, at low water:rock ratios, only a small amount of Fe(II) from the initial harz-

burgite minerals has to be converted into magnetite in order to produce H₂ concentrations that are high enough to stabilize the higher levels of Fe in brucite and serpentine.

3.2.2. Variation with water:rock ratio at 300 °C

Equilibrium mineral assemblages and fluid compositions as a function of water:rock ratio at a constant temperature of 300 °C are shown in Fig. 6. Again, serpentine dominates the equilibrium mineral assemblage over the entire range of W:R studied, accompanied by lesser amounts of brucite, magnetite, and secondary diopside (Fig. 6a). The relative proportions of the minerals in the equilibrium assemblage are fairly constant, although the relative amounts of brucite and diopside are slightly greater and that of magnetite slightly less at lower water:rock ratios. Over the entire range of W:R, the proportions of Fe in both serpentine and brucite are lower than it was in the initial reactant minerals, and the Fe contents increase with decreasing water:rock ratios (Fig. 6c). The pH of the solution is essentially constant for all W:R except for very high values, reflecting control by the mineral assemblage (Fig. 6b). The relative proportion of dissolved elements in the fluid at equilibrium remain essentially constant over most of the range of W:R, but total concentrations increase slightly with decreasing water:rock ratios as incorporation of a larger fraction of water into the alteration minerals focuses solutes in the aqueous phase (Figs. 5b and 6d).

The relatively low Fe contents of serpentine and brucite attained at equilibrium means that a large fraction of Fe is partitioned into magnetite, generating substantial amounts of H₂. As was observed in the 100 °C results, the amount of H₂ generated per kg of harzburgite is greater at higher W:R (Fig. 5a), but the resulting concentration in the fluid decreases with increasing water:rock ratio (Fig. 6b). However, even at high W:R, H₂ concentrations at this temperature are higher than the highest concentrations attained at lower temperatures (e.g., Fig. 4b). At high ratios (W:R > ~5), the equilibrium concentration is below 100 mmolal, but concentrations increase steeply at lower ratios, with calculated equilibrium concentrations exceeding one molal for W:R < ~0.4.

Although the model calculations predict that extremely high H₂ concentrations would be present at equilibrium for very low W:R (Fig. 5b), it is unlikely that such high concentrations would be attained in natural systems, for two reasons. First, the calculated concentrations exceed the solubility of H₂ in high temperature fluids at moderate pressures (Seward and Franck, 1981). For example, at 35 MPa and 300 °C the solubility of H₂ in pure water is about 1.2 molal. As a consequence, alteration of rocks to equilibrium at low water:rock ratios at shallow levels in the crust should lead to exsolution of a separate H₂-rich vapor phase after attaining saturation concentrations. The exact concentration at saturation will depend on a number of factors, including pressure, temperature, fluid salinity, and abundance of other volatiles. However, if saturation and exsolution of a separate H₂ gas phase should occur, the aqueous concentration would then remain essentially constant and equilibrium Fe contents of mineral solid solutions would be lower than those shown in Fig. 5b.

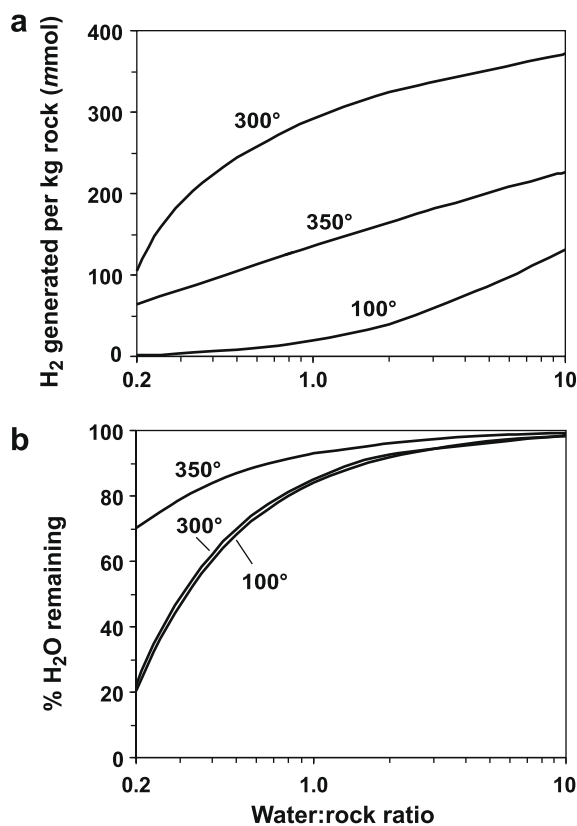


Fig. 5. Amount of H₂ generated per kg harzburgite (a) and percent of the initial H₂O remaining at equilibrium (b) as a function of water:rock ratio. The amount of H₂ generated is expressed as mmoles per kg initial rock.

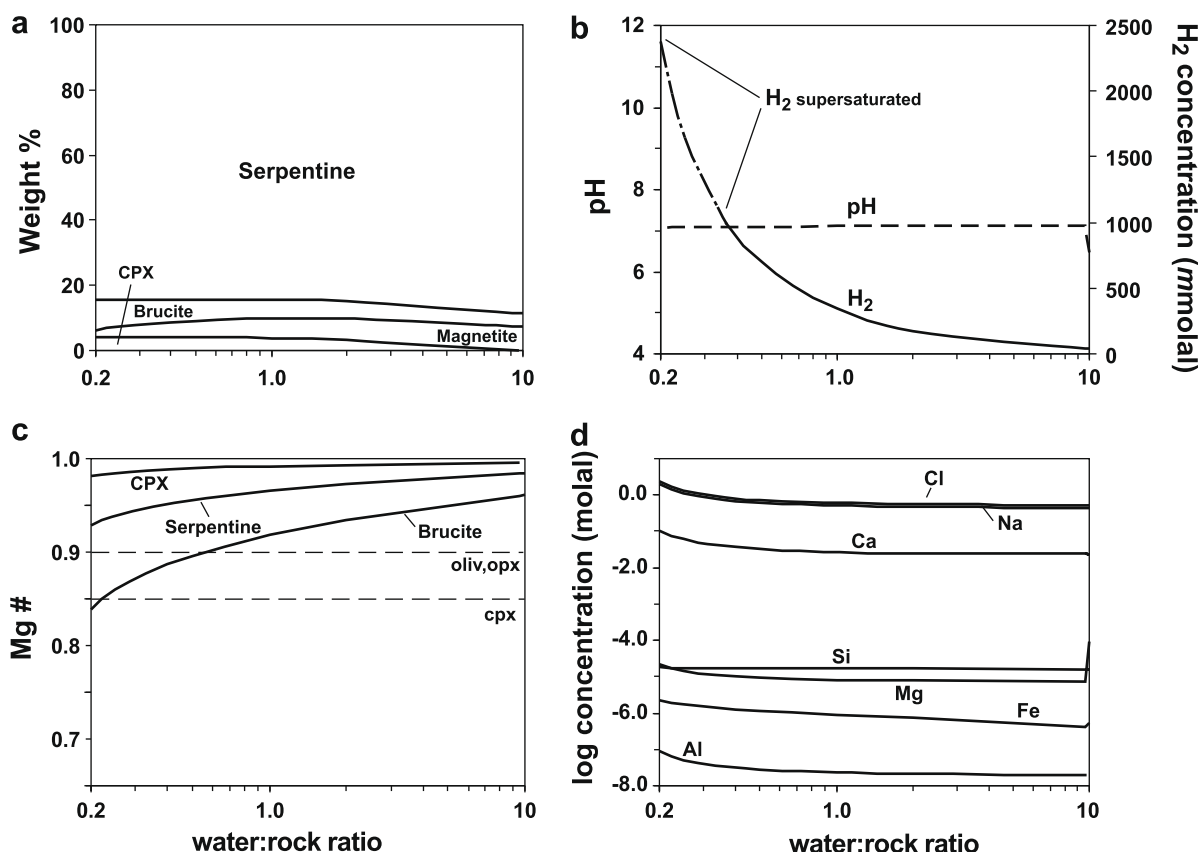
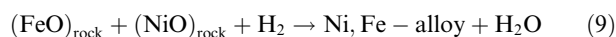
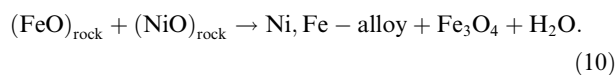


Fig. 6. Predicted equilibrium mineral and fluid compositions for hydrothermal alteration of harzburgite at 300 °C over a range of water:rock ratios. (a) Weight percent of minerals in the alteration assemblage, (b) pH and H₂ concentrations, (c) solid solution compositions, and (d) fluid composition. Dashed lines in (c) indicate composition of minerals in the original harzburgite.

Second, accumulations of high concentrations of H₂ may lead to conditions that are sufficiently reducing to stabilize native metals, particularly Ni,Fe-alloys such as awaruite (Frost, 1985). Once these levels are reached, H₂ generated during magnetite formation will be consumed in the formation of Ni,Fe-alloy through reactions such as:



where (FeO)_{rock} and (NiO)_{rock} represent ferrous iron and nickelous nickel derived from olivine and pyroxene. Alternatively, the overall process can be viewed as a disproportionation of Fe(II) from the ultramafic rocks into both more oxidized and more reduced forms:



Either way, the result is that accumulations of high levels of dissolved H₂ will be limited by formation of native metals, particularly Fe-bearing alloys.

Owing to a lack of thermodynamic data for native metal alloys, it is difficult to place quantitative constraints on the limitations on H₂ concentrations imposed by saturation with respect to Ni,Fe-alloy, or on the amounts of alloys that would be precipitated at equilibrium under hydrothermal conditions. However, Frost (1985) estimated that awaruite is only stable at oxygen fugacities below about

10^{-39.8} at 300 °C and 200 MPa, which is equivalent to dissolved H₂ concentrations above ~340 mmolal. The presence of sulfides can buffer H₂ concentrations at somewhat higher levels (e.g., Alt and Shanks, 1998). Although the exact H₂ concentrations required to stabilize metal alloys and sulfides may be sensitive to pressure and other factors, these considerations suggest that H₂ levels during serpentinization at temperatures around 300 °C and low W:R may level off at around 400 mmolal as concentrations are buffered by mineral assemblages that include native metals and Ni,Fe-sulfide minerals.

3.2.3. Variation with water:rock ratio at 350 °C

Equilibrium mineral assemblages and fluid compositions as a function of water:rock ratio at a constant temperature of 350 °C are shown in Fig. 7. At this temperature, olivine joins serpentine as the predominant members of the equilibrium mineral assemblage for all water:rock ratios, along with lesser amounts of magnetite and secondary diopside (Fig 7a). The proportions of serpentine and magnetite in the equilibrium assemblage decrease somewhat at lower W:R, reflecting the decreasing amount of olivine that must react in order to bring the fluid into equilibrium with the mineral assemblage at lower ratios. Because olivine constituted 80 wt% of the initial harzburgite, between 35% and 55% of the original olivine is converted into alteration

minerals before reaching equilibrium at this temperature, depending on water:rock ratio. For all values of W:R, the Fe content of serpentine is predicted to be less than that of the original olivine and pyroxenes, and increases slightly at lower W:R (Fig. 7c). The pH is constant at ~6.5 over the range of W:R except at very high values, reflecting buffering by the equilibrium mineral assemblage of olivine + serpentine + magnetite + diopside (Fig. 7b). The concentrations of all dissolved elements increase gradually at lower water:rock ratios as an increasing proportion of the water is taken up in hydrated minerals (Fig. 7d).

Equilibrium concentrations of dissolved H₂ exhibit a trend of increasing concentrations at lower water:rock ratios similar to that observed at 300 °C, although the overall concentrations are substantially lower (i.e., ~20–450 mmolal at 350 °C vs. ~40 to >2500 mmolal at 300 °C). The lower overall concentrations at 350 °C relative to 300 °C are attributable to two factors. First, because olivine is only partially reacted at equilibrium, less magnetite is formed and, consequently, the amount of H₂ generated from each kg of harzburgite is significantly lower (Fig. 5a). Second, because a lower proportion of the initial water is incorporated into alteration minerals for an equivalent W:R at 350 °C than at 300 °C (Fig. 5b), H₂ and other dissolved solutes are less concentrated by loss of water.

3.3. Dependence on estimated thermodynamic properties of brucite solid solution

The strong dependence of the predicted equilibrium concentrations of H₂ on the amount of Fe(II) incorporated into solid solutions raises the issue of the sensitivity of the model results to the thermodynamic parameters employed in the calculations, particularly the Fe component of brucite. With regard to the parameters employed for brucite solid solution, uncertainties arise from the values of ΔG°_f , S° and C_p used in the calculations for the endmembers as well as the presumption of ideal mixing behavior for the standard solution. Because the heat capacity makes only a relatively small contribution to the value of the standard Gibbs energy at elevated temperature and pressure ($\Delta G^{\circ}_{T,P}$; Johnson et al., 1992) of Fe(OH)₂ over the temperature range of this study, uncertainties in the assumed values of C_p for this component have only a small impact on the model results. For instance, increasing the assumed C_p for Fe(OH)₂ by 10% decreases $\Delta G^{\circ}_{T,P}$ only slightly from $-518.3 \text{ kJ mol}^{-1}$ to $-519.0 \text{ kJ mol}^{-1}$ at 250 °C and 35 MPa. Additional model calculations (not shown) performed with the C_p for Fe(OH)₂ varied by $\pm 10\%$ from the value adopted in this study resulted in predicted amounts of minerals, Mg#s for solid solutions, and H₂ con-

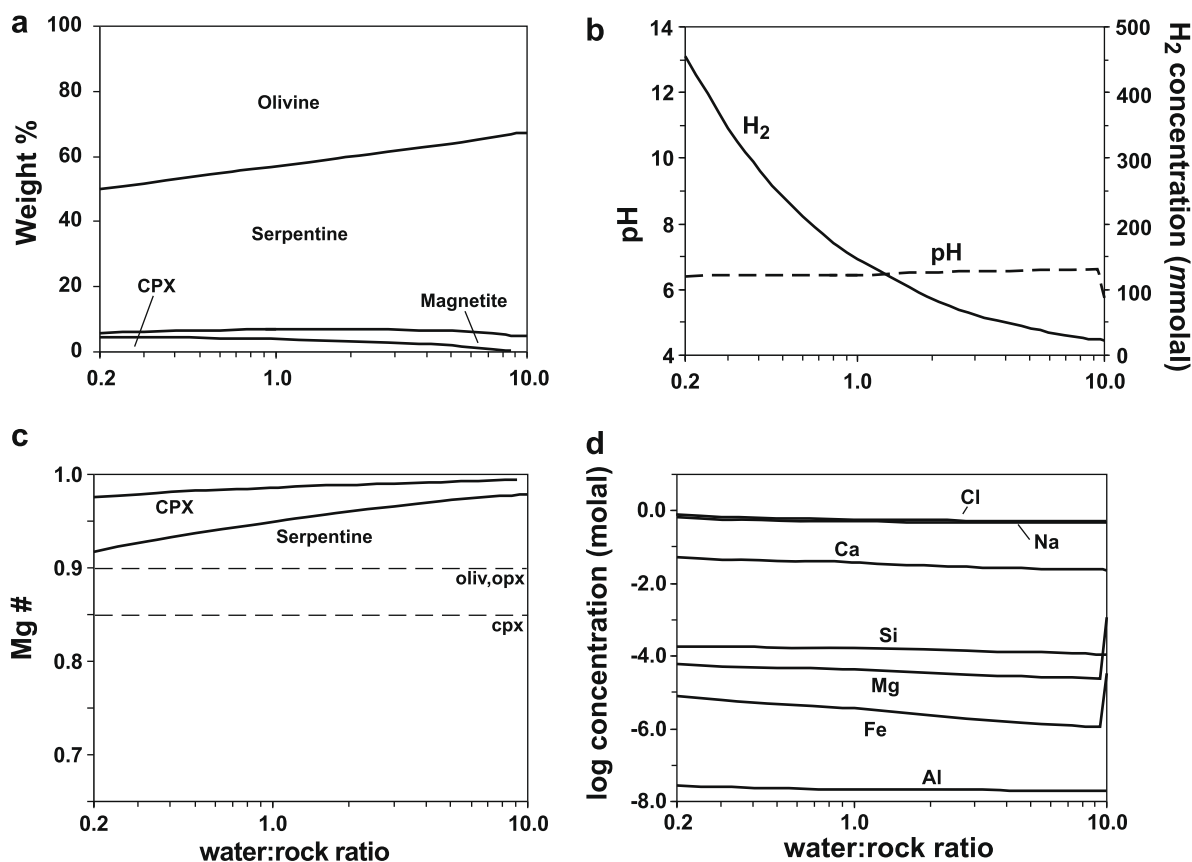


Fig. 7. Predicted equilibrium mineral and fluid compositions for hydrothermal alteration of harzburgite at 350 °C over a range of water:rock ratios. (a) Weight percent of minerals in the alteration assemblage, (b) pH and H₂ concentrations, (c) solid solution compositions, and (d) fluid composition. Dashed lines in (c) indicate composition of minerals in the original harzburgite.

centrations that deviated by <3% from the results presented above.

More substantial variations may arise from the value of $\Delta G_{f,Fe(OH)_2}^\circ$ adopted in the calculations. The value employed here ($-492.82 \text{ kJ mol}^{-1}$) is taken from Sverjensky and Molling (1992), which is derived from solubility data for $Fe(OH)_2$ reported by Baes and Mesmer (1976). The value from Sverjensky and Molling (1992) is in agreement within the stated uncertainty ($\pm 4 \text{ kJ mol}^{-1}$) with that derived for $Fe(OH)_2$ by Refait et al. (1999) ($-490 \pm 1 \text{ kJ mol}^{-1}$), but differs more considerably from the value reported by Wagman et al. (1982) ($-486.5 \text{ kJ mol}^{-1}$).

In order to assess the potential impact of the adopted value of $\Delta G_{f,Fe(OH)_2}^\circ$ on the outcome of the models, additional calculations were performed substituting the $\Delta G_{f,Fe(OH)_2}^\circ$ value from Wagman et al. (1982) for $Fe(OH)_2$ while leaving all other thermodynamic parameters unchanged. A comparison of selected results from these calculations is shown in Fig. 8, where it can be seen that the models performed with the value from Wagman et al. (1982) predict much lower Fe contents for brucite at equilibrium for all temperatures, along with substantially larger amounts of magnetite and H_2 concentrations. Indeed, Mg#s for brucite remain above 0.93 at all temperatures in the models using the Wagman et al. datum. If the Wagman et al. value is accurate, the model predictions presented above may substantially overestimate the role of Fe partitioning into brucite and the amount of H_2 generated during incipient serpentinization. However, the low levels of Fe in brucite predicted in the model using the Wagman et al. data would appear to be inconsistent with observations of Fe-rich brucite in natural samples (Hostetler et al., 1966; Page, 1967; Moody, 1976a,b; D'Antonio and Kristensen, 2004; Bach et al., 2006) and laboratory experiments (Moody, 1976b; Allen et al., 1995; Seyfried et al., 2007).

The above comments notwithstanding, it should be kept in mind that inaccurate predictions of equilibrium Fe partitioning and H_2 concentrations may also arise from uncertainties in the thermodynamic data for components other than $Fe(OH)_2$, even those that do not contain Fe. For example, uncertainties in the thermodynamic data for pure Mg-brucite and magnetite are both of a similar magnitude to that of $Fe(OH)_2$ (Helgeson et al., 1978), and could potentially lead to inaccurate predictions of the same magnitude as that produced by variations in the reported values of $\Delta G_{f,Fe(OH)_2}^\circ$. As a consequence, it should not be assumed that the estimated thermodynamic parameters for $Fe(OH)_2$ are the only, or even the most substantial, source of potential errors in the calculations.

4. PHYSICAL AND CHEMICAL IMPLICATIONS

The thermodynamic models presented above emphasize that the partitioning of Fe among alteration minerals will exert a strong influence on the amount of H_2 generated during aqueous alteration of ultramafic rocks. In particular, partitioning of Fe(II) into serpentine and brucite can significantly reduce the amount of magnetite produced during

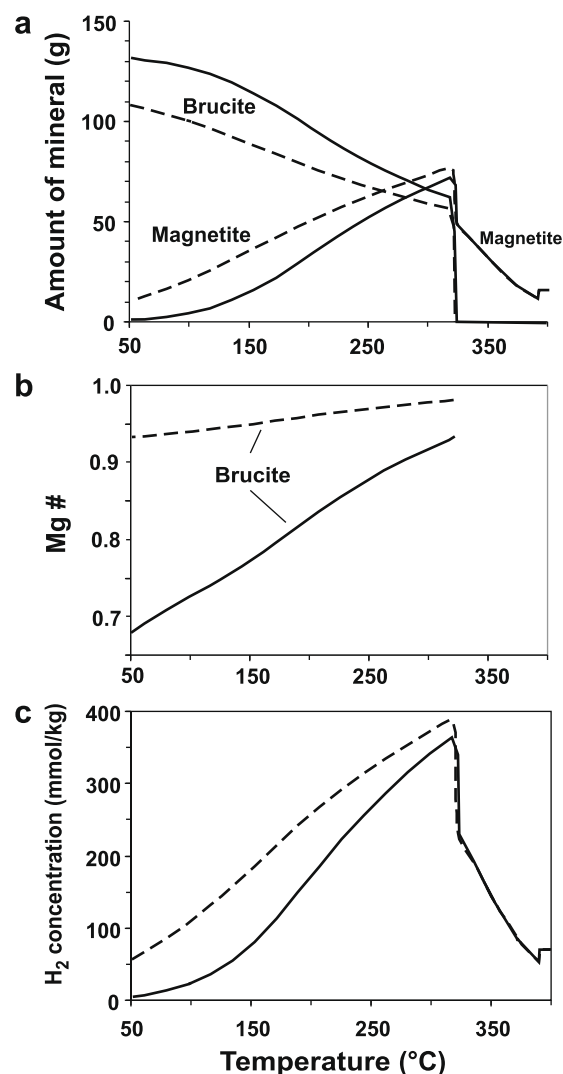


Fig. 8. Comparison of selected model results for calculations using the thermodynamic database employed in the present study (solid lines) with calculations performed using data for $Fe(OH)_2$ from Wagman et al. (1982) (dashed lines). (a) Equilibrium amounts of brucite and magnetite generated per kilogram harzburgite reacted. (b) Brucite solid solution compositions. (c) H_2 concentration.

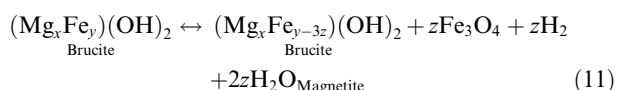
alteration and, consequently, the amount of H_2 generated. Furthermore, the models predict that reaction temperature has a particularly large impact on the proportion of Fe(II) that precipitates as a component of brucite, with the Fe content increasing substantially at lower reaction temperatures. Water:rock ratio also influences the Fe content of brucite somewhat, but the impact of this factor is relatively minor compared to that of reaction temperature. In contrast, temperature apparently has only a modest impact on the Fe content of serpentine. Nevertheless, the partitioning of Fe(II) into serpentine minerals can significantly reduce the amounts of magnetite and H_2 that would be formed if all Fe was excluded from the mineral during alteration.

The range of brucite compositions predicted by the geochemical models (Mg# ≈ 0.7 – 0.95) appears to be consistent

with the range of compositions observed in natural serpentinites (e.g., Hostetler et al., 1966; Page, 1967; Moody, 1976a; D'Antonio and Kristensen, 2004; Bach et al., 2006) as well as the limited data available from laboratory experiments (Moody, 1976b; Allen and Seyfried, 1995; Seyfried et al., 2007). The models also predict an increase in Fe content of brucite with decreasing temperature, which appears to agree with trends observed in the limited experimental data available for lower temperature alteration of Fe-bearing olivine (Moody, 1976b; Seyfried et al., 2007). The predicted compositions of serpentine ($Mg\# \approx 0.92$ – 0.96) are also comparable to those in natural serpentinites, which are generally depleted in Fe by several mole% relative to the original olivine and pyroxene in the precursor rock (e.g., Früh-Green et al., 1996; Mevel and Stamoudi, 1996). Although it is uncertain whether variable amounts of Fe in natural serpentinization products reflect equilibrium or metastable partitioning, it is apparent that Fe content in brucite plays a fundamental role in the extent of magnetite and H_2 formation.

At low temperatures, the thermodynamic constraints on H_2 generation will be compounded by kinetic factors that further limit rates of H_2 generation from serpentinizing rocks. While there are many factors that influence reaction rates, it appears that reaction rates are sufficiently rapid at temperatures $> \sim 200$ °C that extensive serpentinization can occur in fluids circulating through ultramafic rocks on timescales of a thousand years or less (Table 4) (Wegner and Ernst, 1983). Conversely, substantially longer timescales are apparently required for serpentinization to proceed at lower temperatures. Thus, unless fluid residence times are very long, the amount of H_2 present in fluids circulating through ultramafic rocks at low temperatures are likely to be restricted both by the partitioning of Fe into brucite and by limited reaction progress owing to kinetic limitations.

While the models predict that ultramafic rocks altered at low temperatures should contain Fe-enriched brucite, the models refer to the initial stage of alteration during reaction of aqueous fluids with fresh ultramafic rocks in a closed system, and the alteration assemblages produced under such conditions may become unstable and undergo further reaction as conditions change. In particular, the stability of Fe-rich brucite depends on the activity of H_2 in the system and, if the H_2 activity decreases, Fe-bearing brucite will become unstable, decomposing to magnetite and brucite with a lower Fe content. That is, loss of H_2 from the system will cause the reaction:



to proceed to the right. Thus, loss of H_2 by fluid advection or diffusion, or a decrease in H_2 activity owing to influx of additional fluids, will cause the Fe(II) component of brucite to be converted into magnetite, reducing the Fe content of the brucite and generating additional H_2 . Over time, most or all of the Fe content of brucite formed during incipient alteration of ultramafic rocks may be converted to magnetite, so that rocks altered

Table 4

Estimated time required for 50% ($t_{50\%}$) and 99% ($t_{99\%}$) serpentinization of olivine in the presence of excess H_2O (data from Wegner and Ernst, 1983).[#]

Temperature (°C)	$t_{50\%}$ (years)	$t_{99\%}$ (years)
20	40,000	270,000
50	13,000	86,000
100	2,900	19,000
150	930	6200
230	240	1600
310	90	600

[#] Data shown are for pure forsteritic olivine with 50 mm grain diameters and a pressure of 50 MPa.

at lower temperatures may eventually evolve to have abundances of magnetite and low-Fe brucite compositions similar to serpentinites formed at much higher temperatures. In serpentinites initially formed at low temperatures, this process may result in a steady source of H_2 as Fe-rich brucite gradually decomposes in response to continual loss of H_2 from the system. In this case, the total amount of H_2 generated from low temperature serpentinites over time could equal the amount generated during higher temperature alteration, although the H_2 generation in this case would be gradual and at consistently lower concentrations.

Initially formed alteration assemblages may also become unstable as the temperature of the system decreases. For instance, ultramafic rocks initially altered at temperatures above ~ 390 °C where olivine is essentially unreactive should contain talc and tremolite as the primary alteration minerals. But, as the temperature of these rocks decrease, they will enter a regime where olivine is increasingly reactive and serpentine plus magnetite should replace olivine and talc as the predominant alteration phases (Fig. 2a). This change in mineral assemblage should be accompanied by steeply increasing concentrations of H_2 , especially when the system approaches the temperature where olivine is no longer stable (~ 315 °C) (Fig. 2). Under closed system conditions, the thermodynamic models would also predict that magnetite formed during serpentinization at higher temperatures should be converted to Fe-rich brucite as temperatures decrease (i.e., Rxn. 11 proceeding to the left) (Fig. 2a). However, natural serpentinites are likely to be open systems, particularly with respect to H_2 , so that cooling systems may not result in conversion of magnetite to Fe-rich brucite, since this reaction requires H_2 to proceed.

While partitioning of Fe(II) into serpentine minerals will also effect the amount of H_2 generated during serpentinization, the models indicate that thermodynamic controls on the partitioning of Fe into serpentine are much less variable than that of brucite. The narrow range of Fe contents predicted by the models ($Mg\# \approx 0.93$ – 0.97) appears to be consistent with the limited variation of Fe in natural serpentinites (e.g., Früh-Green et al., 1996, 2004; Mével and Stamoudi, 1996). Nevertheless, even a small amount of Fe(II) partitioning into serpentine can substantially re-

duce the overall amount of H_2 generated during serpentinization.

The thermodynamic models also indicate that diopside clinopyroxene can be a stable member of the equilibrium mineral assemblage over a broad range of temperatures during hydrothermal alteration of peridotites. Relict clinopyroxene is commonly observed in ultramafic rocks that have undergone serpentinization, where its presence is accounted for by the inference that clinopyroxene alteration occurs at a slower rate than that of orthopyroxene and olivine. However, the thermodynamic models suggest a different interpretation is possible. The clinopyroxene may persist simply because it becomes thermodynamically stable in equilibrium with the other minerals and fluid present. If this is the case, then the persistence of clinopyroxene may be due to thermodynamic rather than kinetic factors, and the inherent reaction rate of clinopyroxene may not be the primary factor responsible for its occurrence in partially serpentinized rocks.

4.1. Stability of native metals and oxidation state during serpentinization

One of the most distinctive aspects of serpentinites is the occurrence in many of these rocks of native metals and metal alloys such as awaruite. Although minor components of the rocks, these metals are of particular interest as indicators of the oxidation state during serpentinization (Frost, 1985; Alt and Shanks, 1998). In addition, Ni,Fe-alloys such as awaruite have been proposed to be catalysts for methane formation during serpentinization (Horita and Berndt, 1999), and may be capable of catalyzing the synthesis of more complex organic compounds as well.

Since metallic elements are present in pristine ultramafic rocks primarily in the +2 oxidation state [e.g., Fe(II), Ni(II)], formation of native metals involves reduction of these elements, which requires very strongly reducing conditions (i.e., high levels of H_2). Curiously, since reducing environments in serpentinites develop from the oxidation of Fe(II), formation of Fe-bearing alloys requires that some Fe(II) in the rocks must first be oxidized in order to create the conditions that allow Fe reduction. This requirement also indicates that, on some scale, native metals must always co-occur with magnetite or some other Fe(III)-bearing mineral. This means that olivine can alter to an assemblage of serpentine + Ni,Fe-alloy \pm brucite only if the serpentine contains significant Fe(III).

Owing to limited availability of thermodynamic data for metal alloys at elevated temperatures and pressures, it is not presently possible to place precise quantitative constraints on the conditions required for their formation. However, it appears that H_2 concentrations of several hundred mmolal H_2 are required in order for Ni,Fe-alloys to be stable, at least for temperatures around 300 °C (Frost, 1985). The model results predict that sufficiently reducing conditions to allow Ni,Fe-alloys to form may only be generated during serpentinization for a limited range of temperature and water:rock ratios. For the modeled rock composition and pressure (35 MPa), H_2 concentrations exceeding a few hundred

mmolal occur only at temperatures of \sim 250 °C to 350 °C and relatively low water:rock ratios. At intermediate temperatures in this range (\sim 300–315 °C), equilibrium H_2 concentrations exceeding several hundred mmolal occur for W:R up to \sim 1 (Fig. 6), but these high concentrations are only attained at much lower W:R (\ll 1) for higher and lower temperatures (Fig. 7).

If these predictions are correct, they indicate that formation of native metals and metal alloys during serpentinization may be limited to a fairly restrictive range of environmental conditions. In particular, the models suggest that metal alloys may only form during the initial stages of fluid penetration while water:rock ratios are low, and should become unstable with continued fluid penetration as effective water:rock ratios increase. Furthermore, awaruite and other Ni,Fe-alloys may only be expected to form in rocks undergoing serpentinization at temperatures between about 250 °C and 365 °C for shallow environments within the ocean crust, and might be absent from rocks undergoing serpentinization at higher and lower temperatures. Ni,Fe-alloy formation may be localized to rocks undergoing serpentinization at peak H_2 -generating temperatures around 300–315 °C. Based on the pressure dependence of serpentine-forming reactions (Fig. 1), these temperatures can be expected to increase by a few tens of degrees for pressures up to 500 MPa.

Frost (1985) noted that awaruite commonly occurs in rocks that are only partially serpentinized, where relict olivine occurs along with serpentine, brucite and magnetite. Results of the thermodynamic models suggest that, at temperatures where olivine is present as a stable member of the equilibrium assemblage ($>$ \sim 315–390 °C), sufficiently reducing conditions to allow awaruite to precipitate only occur at very low water:rock ratios (e.g., Fig. 7). Under these conditions, however, brucite is not a member of the equilibrium assemblage. At lower temperatures where olivine is unstable but brucite occurs as an alteration phase, H_2 concentrations that would allow awaruite to form appear to occur over a much larger range of water:rock ratios (Fig. 6).

These considerations suggest two possible scenarios for the co-occurrence of awaruite and olivine in rocks of harzburgitic composition. First, the awaruite may form at temperatures above 315 °C at very low W:R, in which case the brucite may represent a metastable transition phase or reflect localized equilibrium owing to fine-scale compositional variations. Second, the awaruite may form at lower temperatures (i.e., \sim 250–315 °C) with the persistence of olivine attributable to kinetic factors or limited water availability. Because the hydration of olivine appears to be very rapid at geologic timescales at these temperatures (e.g., Table 4; Wegner and Ernst, 1983), it seems unlikely that the kinetics of mineral reactions would be responsible for relict olivine. Instead, it seems more likely that the persistence of olivine would be related to slow penetration of water to the reacting mineral surface or to infiltration of insufficient water to completely hydrate the rock. The processes may be interrelated, since alteration may allow further penetration of fluids to the unreacted olivine surface. In either case, it appears likely that awaruite formation may occur predominantly under very low effective water:rock ratios, even at

temperatures where olivine is not thermodynamically stable in the presence of aqueous solutions.

Frost (1985) also noted that metal alloys appear to be preferentially associated with the “serpentinization front” and disappear as serpentinization progresses away from this front according to the sequence: (1) partially serpentinized harzburgite + awaruite → (2) serpentine + awaruite → (3) serpentine + magnetite. This observation would appear to be somewhat incongruous, since it would be expected that more extensive serpentinization and magnetite formation would generate greater amounts of H_2 and therefore more strongly reducing conditions favoring awaruite formation. Frost (1985) suggested that this sequence can be interpreted as a non-equilibrium process in which the most strongly reducing conditions occur during active serpentinization of olivine and then evolve to less reducing conditions once the reaction is complete. Alternatively, the models suggest that this reaction sequence might represent equilibrium relations over a range of effective water:rock ratios. At the serpentinization front, a large fraction of the infiltrating water is adsorbed into hydrated minerals, creating extremely low effective water:rock ratios. The H_2 generated is focused into the remaining fluid to high H_2 activity, stabilizing awaruite and, possibly, Fe-rich brucite. Behind this front, however, continued fluid infiltration means that the rock communicates with a larger reservoir of fluid and experiences a higher effective water:rock ratio, diluting the H_2 generated to lower concentrations, and destabilizing awaruite and Fe-rich brucite in favor of magnetite. Consequently, awaruite may form during initial penetration of water into fresh rock, but then become unstable with continued infiltration, while maintaining local equilibrium throughout. Yet another possibility is that the reaction sequence reflects diffusion of H_2 away from the reaction front. Whatever the reaction path, even in partially serpentinized rocks awaruite must be associated on some scale with magnetite or some other Fe(III)-bearing phase to supply sufficient H_2 to stabilize the alloy.

4.2. Implications for timing of magnetite formation and magnetization of the ocean crust

Formation of magnetite during serpentinization of peridotites significantly alters the rock's magnetic properties, and hence has implications for the role of serpentinites in oceanic magnetic anomalies and evolution of the magnetization of the ocean crust (e.g., Toft et al., 1990; Dyment et al., 1997; Oufi et al., 2002; Bach et al., 2006). Several aspects of the model results have potential implications for interpreting the timing and extent of magnetite formation during alteration of ultramafic rocks. First, during incipient alteration, the amount of magnetite formed appears to be strongly influenced by the reaction temperature (Fig. 2a), so that the greatest extent of magnetite formation should occur at temperatures around 300–315 °C, with lesser amounts of magnetite produced during initial alteration of fresh rock at both higher and lower temperatures. At low temperatures, inhibition of magnetite formation by partitioning of Fe into brucite and serpentine will be compounded by slow reaction kinetics (Table 4). Accordingly,

the strongest and most rapid increase in magnetization should occur in fresh rocks that undergo initial serpentinization at around 300 °C.

Over time, however, the amount of magnetite formed in rocks initially altered at temperatures above and below this optimal range may increase substantially. At temperatures $> \sim 315$ °C, where olivine is partially or entirely persistent at equilibrium, only small amounts of magnetite should form during initial alteration. But, as such systems cool, the remaining olivine should increasingly react and the amount of magnetite produced should therefore increase steadily (Fig. 2a), more strongly effecting the magnetization of the crust. At lower temperatures ($< \sim 250$ °C), alteration of pristine ultramafic rocks should initially produce Fe-rich brucite with only modest amounts of magnetite (Fig. 2a). However, loss of H_2 from the system through either advection or diffusion will destabilize the Fe component of brucite and cause it to decompose to magnetite. As a consequence, ultramafic rocks that undergo serpentinization at low temperatures can be expected to generate increasing amounts of magnetite and stronger magnetization over time. The rate of this process would depend on the rate of H_2 loss from the rocks, such that the timing of increased magnetization of the crust may be largely controlled by fluid advection or diffusive processes. Furthermore, at these temperatures the kinetics of reactions may be sufficiently slow that these reactions would require significant amounts of time, so that increased magnetization from decomposition of Fe-rich brucite might proceed only gradually as the crust ages.

The model results also indicate that magnetite formation and magnetization should increase with increasing water:rock ratio during alteration (Figs. 4, 6 and 7). As a result, initial penetration of fluids into fresh rock can be expected to produce limited amounts of magnetite, particularly at lower temperatures. As fluid fluxes and integrated water:rock ratios increase, more magnetite should be produced resulting in increased magnetization. Even rocks that have undergone pervasive serpentinization under low water:rock ratio conditions may exhibit an increase in magnetite formation with continued fluid penetration as these fluids lower H_2 concentrations through dilution and lead to destabilization of Fe-rich brucite in favor of magnetite (i.e., by driving Rxn. 7 to the right).

Trends in magnetic susceptibility as a function of density in the ocean crust indicate that magnetite primarily forms when the density is already low (that is, after most of the rock is already serpentinized). Density-magnetic susceptibility relations indicate that the production of magnetite is limited in most rocks until they have been 60–70% serpentinized (Toft et al., 1990; Oufi et al., 2002; Frost and Beard, 2007). These trends suggest that Fe-rich brucite forms during incipient serpentinization of the rocks and is subsequently replaced by magnetite, a reaction sequence further supported by recent TEM results (Bach et al., 2006). One interpretation of this observation that is consistent with the model results is that the rocks undergo serpentinization at temperatures and low water:rock ratios where Fe-rich brucite is stable relative to magnetite, and then the magnetite “grows in” as H_2 activity decreases,

either by migration of H_2 out of the rocks by diffusion/advection or by dilution during intrusion of additional fluids. If this is the case, the rate of diffusion (or advection) of H_2 from serpentinized rocks may play a prominent role in controlling the timing of the development of increasing magnetization of the oceanic crust as it ages.

4.3. Implications for hydrogen-based microbial communities and abiotic organic synthesis

The H_2 generated during serpentinization can potentially support populations of autotrophic microorganisms in two types of environments. First, if temperatures are low enough to allow life, hydrogen-consuming organisms can inhabit the interior of ultramafic rocks and take advantage of H_2 generated by serpentinizing reactions in their immediate surroundings. Second, organisms can inhabit environments where H_2 -rich fluids discharge from serpentinites and are exposed to seawater or the atmosphere (Kelley et al., 2001, 2005; Takai et al., 2004; McCollom, 2007). In either case, the capacity for the environment to support hydrogen-consuming microorganisms depends on the amount and rate of H_2 generated during serpentinization.

In environments with temperatures low enough for life to exist ($< \sim 130^\circ\text{C}$), the models indicate that partitioning of Fe into brucite may significantly restrict the amount of H_2 produced during serpentinization. At the same time, kinetic inhibitions will hamper the progress of serpentinization reactions, perhaps requiring many thousands of years for a given piece of rock to be completely serpentinized (Table 4). If these effects are combined, the rate of supply of H_2 to organisms within low temperature serpentinites could be severely limited. Considering that the strongly alkaline conditions attained during low temperature serpentinizing may impose steep metabolic costs or nutrient limitations in addition to a limited H_2 supply, the interiors of serpentinizing rocks could be very challenging environments for hydrogen-consuming organisms to inhabit. Despite these potential limitations, indirect evidence that microbial life exists within serpentinites beneath the seafloor is provided by analyses of sulfur isotopes in drill cores which indicate that sulfate reducing microorganisms have contributed significant sulfur to the rocks (Alt and Shanks, 1998; Alt et al., 2007).

Hydrogen-enriched hydrothermal fluids associated with ultramafic rocks have been observed discharging from the seafloor at several locations, including both high temperature hydrothermal systems along the axis of the mid-ocean ridge (Charlou et al., 1998, 2002; Takai et al., 2004) and moderate temperature systems off-axis (Kelley et al., 2001, 2005). Both types of environments support substantial autotrophic microbial communities of which hydrogen-consuming organisms appear to constitute a major component (e.g., Miroshnichenko et al., 2003a,b; Schrenk et al., 2004; Takai et al., 2004; Kelley et al., 2005; Voordeckers et al., 2005; Brazelton et al., 2006). Hydrogen-rich alkaline springs have also been observed discharging from serpentinites on land (Barnes and O'Neil, 1969; Neal and Stanger, 1983; Abrajano et al., 1988, 1990), but the microbial com-

munities associated with these springs are just beginning to be explored (Johnson et al., 2006).

High temperature ($352\text{--}365^\circ\text{C}$) hydrothermal vent fluids whose chemical compositions suggest interaction with ultramafic rocks in the subsurface have been identified at several sites along the mid-ocean ridge, including Rainbow, Logatchev, and Kairei (Charlou et al., 1998, 2002; Takai et al., 2004). Measured H_2 concentrations in these fluids range from 2.5 to 16 mmolal, and are the highest concentrations reported for steady-state, unconsolidated mid-ocean ridge hydrothermal vents. At their measured venting temperatures, these systems should be in a regime where olivine is reactive (Fig. 2). However, the fluids may have cooled during transport to the surface, and temperatures within subsurface reaction zones may be higher than the observed venting temperatures. For example, Allen and Seyfried (2003) have suggested that fluid compositions at Rainbow may be controlled by reaction at temperatures above 400°C . In such circumstances, the fluid-rock interactions that control fluid compositions in these systems may be taking place at temperatures where olivine is stable, with the primary alteration products being talc, tremolite, and magnetite rather than serpentine (Fig. 2; Allen and Seyfried, 2003).

If this is the case, it suggests the possibility that vent fluid H_2 concentrations in these systems might increase over time if the systems cool and temperatures in the reaction zone decrease to the point where olivine becomes unstable. The model results suggest that reaction zone temperatures in the vicinity of $\sim 300\text{--}325^\circ\text{C}$ would generate the highest concentrations of H_2 , potentially attaining concentrations an order of magnitude or more higher than those yet observed in seafloor systems. To date, however, no fluids have been obtained from systems within this optimal temperature range for H_2 generation. Nevertheless, the presence of Ni,Fe-alloys in some seafloor serpentinites (e.g., Alt and Shanks, 1998) suggests that fluids with very high H_2 concentrations occur within the ocean crust in some circumstances, and these fluids may at times vent to the seafloor. Such systems would have an ever greater potential to support populations of hydrogen-consuming organisms than the currently recognized sites.

Moderate temperature ($40\text{--}91^\circ\text{C}$) hydrothermal fluids with H_2 concentrations up to 15 mmolal have also been reported off-axis at the Lost City site (Kelley et al., 2001, 2005). Similar to the higher temperature systems, it appears that the hydrothermal fluids at this location originate from reaction zones in the subsurface that are at higher temperatures than those measured at the seafloor. Estimated subsurface temperatures for the Lost City system are $\sim 110\text{--}200^\circ\text{C}$ (Allen and Seyfried, 2003; Proskurowski et al., 2006), and in this temperature range the model results suggest that H_2 concentrations may be limited by formation of Fe-rich brucite. To date, brucite has not been reported in basement rocks collected from exposures adjacent to the Lost City hydrothermal vents (e.g., Kelley et al., 2005; Boschi et al., 2006), but these rocks may not reflect conditions in the subsurface.

In addition to high levels of H_2 , fluids venting from serpentinites are commonly observed to have high

abundances of methane and other hydrocarbons (e.g., Abrajano et al., 1988, 1990; Charlou and Donval, 1993; Charlou et al., 1998, 2002; Holm and Charlou, 2001; Kelley et al., 2001, 2005; Proskurowski et al., 2008). The occurrence of these compounds has often been attributed to abiotic organic synthesis from reduction of CO₂ (or bicarbonate) during serpentinization, perhaps involving mineral catalyzed processes analogous to Fischer–Tropsch synthesis. The overall process can be expressed by the general reaction:



Experimental studies support the potential for methane and other light hydrocarbons to form by reduction of CO₂ under conditions that can occur during serpentinization (e.g., Horita and Berndt, 1999; McCollom and Seewald, 2001, 2003, 2007; Foustoukos and Seyfried, 2004; Seewald et al., 2006; Fu et al., 2007).

Because the abiotic formation of organic compounds according to Rxn. 12 requires H₂, the reaction can, in general, be expected to be more favorable under conditions that generate higher concentrations of H₂. According to the model predictions, rocks undergoing serpentinization in the 200–315 °C range should generate the greatest amounts of H₂, and would therefore appear to have the greatest potential as environments for abiotic organic synthesis. Similarly, lower water:rock ratios should provide more favorable conditions for abiotic synthesis. Of course, other factors such as the abundance and speciation of inorganic carbon, residence time, and occurrence of potential catalysts will also effect abiotic synthesis reactions, and would have to be considered when comparing the relative potential for organic synthesis between specific environments.

Serpentinization in the 200–315 °C temperature range might also promote abiotic organic synthesis in two additional ways. First, reduction of dissolved CO₂ to methane is kinetically inhibited at temperatures below about ~400 °C, so that production of methane is sluggish even under highly favorable circumstances (McCollom and Seewald, 2001, 2003, 2007; Foustoukos and Seyfried, 2004; Seewald et al., 2006). However, the reaction can be effectively catalyzed by Ni,Fe-alloys, and rapid reduction of CO₂ to methane in the presence of Ni,Fe-alloy has been observed experimentally at temperatures as low as 200 °C (Horita and Berndt, 1999). As discussed above, Ni,Fe-alloys require very strongly reducing conditions to form, and may occur only in ultramafic rocks undergoing serpentinization under a limited range of conditions (perhaps between 200 °C and 315 °C and W:R < ~1). Where it does occur, the combination of high H₂ abundance and an effective catalyst will provide a very favorable environment for methane synthesis. Such environments, however, may not be widespread, and none of the deep sea hydrothermal systems associated with ultramafic rocks that have been observed to date have sufficiently high H₂ concentrations to stabilize Ni,Fe-alloys. Consequently, it appears unlikely that methane synthesis catalyzed by Ni,Fe-alloys is currently taking place in these systems, unless it is occurring in parts of the system where H₂ levels are higher than those reflected in the vent fluids.

Second, while reduction of dissolved CO₂ appears to be relatively sluggish even in the presence of potential catalysts such as magnetite and chromite, reduction of gas phase CO₂ may proceed much more rapidly (see McCollom and Seewald, 2007). Consequently, conditions within serpentinites that produce a separate gas phase may promote abiotic organic synthesis reactions. In shallow systems, separation of a gas phase may occur by boiling as the fluids migrate upward through the crust. In deeper systems, saturation of the fluids with respect to H₂ may lead to separation of an H₂-rich gas phase. At 35 MPa, H₂ saturation in pure water ranges from ~0.4 mol% at 100 °C to ~3 mol% at 350 °C, approximately equivalent to concentrations of 220 and 1660 mmolal (Seward and Franck, 1981). According to the model predictions, H₂ concentrations approaching saturation could potentially be attained during serpentinization at temperatures of ~250–315 °C and W:R < ~0.5 ratios for the pressure of the models (35 MPa), suggesting the possibility that a separate H₂-rich gas phase favorable for organic synthesis could form in some serpentinites.

5. CONCLUDING REMARKS

The thermodynamic models presented here are an initial attempt at constraining the factors that control H₂ generation during hydrothermal alteration of ultramafic rocks. Strictly speaking, the models are only applicable to the conditions of the calculations, and different conditions in natural environments (rock and fluid compositions, pressure, closed- vs. open systems, etc.) may cause variations from the equilibrium predictions made in the present models. Nevertheless, it appears likely that the impact of these variations will be comparatively modest, and most of the conclusions will be broadly applicable to alteration of ultramafic rocks in general, even if the details deviate somewhat from the present predictions. The models themselves can be readily adapted to conditions beyond those explored here in order to make more detailed interpretations of specific geologic situations. Overall, the results demonstrate that thermodynamic reaction path models can be a useful tool to investigate geochemical processes during alteration of ultramafic rocks.

The models also reveal some significant limitations in the data currently available to conduct theoretical assessments of the hydrothermal alteration of ultramafic rocks. In particular, the models in this study required use of estimated thermodynamic parameters for several Fe-bearing solid solutions, including those for brucite and serpentine. Also, while Ni-bearing minerals such as awaruite and heazlewoodite are commonly used as indicators of oxidation state during serpentinization of ultramafic rocks (e.g., Frost, 1985; Alt and Shanks, 1998), current thermodynamic databases do not include parameters for these minerals, precluding inclusion of Ni-bearing phases without investment of substantial additional effort. Attainment of more complete and accurate thermodynamic data for Fe- and Ni-bearing phases in the future would allow for more accurate models and broaden the range of applications of the model predictions. In addition, improved understanding

of the relative and absolute reaction rates for the minerals involved would allow the relative contributions of thermodynamics and kinetics on mineral alteration and H₂ generation to be considered (e.g., Seyfried et al., 2007).

ACKNOWLEDGMENTS

This study was completed with funds provided by the NASA Astrobiology Institute through a cooperative agreement with the University of Colorado and by NSF Ocean Science Division grant OCE0550800. Helpful reviews by Gretchen Früh-Green, Bill Seyfried, and an anonymous reviewer, as well as the efforts of the associate editor, are gratefully appreciated.

REFERENCES

- Abrajano T. A., Sturchio N. C., Bohlke J. K., Lyon G. L., Poreda R. J. and Stevens C. M. (1988) Methane–hydrogen gas seeps, Zambales Ophiolite, Philippines: deep or shallow origin? *Chem. Geol.* **71**, 211–222.
- Abrajano T. A., Sturchio N. C., Kennedy B. M., Lyon G. L., Muehlenbachs K. and Bohlke J. K. (1990) Geochemistry of reduced gas related to serpentinization of the Zambales ophiolite, Philippines. *Appl. Geochem.* **5**, 625–630.
- Allen D. E. and Seyfried, Jr., W. E. (2003) Compositional controls on vent fluids from ultramafic-hosted hydrothermal systems at mid-ocean ridges: an experimental study at 400 °C, 500 bars. *Geochim. Cosmochim. Acta* **67**, 1531–1542.
- Allen D. E., Berndt M. E. and Seyfried Jr. W. E. (1995) Iron component of brucite as an indicator of fH₂ during serpentinization of olivine at 300 °C and 500 bars. *EOS Trans. AGU*, **76**, Fall Meeting Suppl., V32B-2 (abstr.).
- Alt J. C. and Shanks, III, W. C. (1998) Sulfur in serpentinized oceanic peridotites: serpentinization processes and microbial sulfate reduction. *J. Geophys. Res.* **103**, 9917–9929.
- Alt J. C. and Shanks, III, W. C. (2003) Serpentinization of abyssal peridotites from the MARK area, Mid-Atlantic Ridge: sulfur geochemistry and reaction modeling. *Geochim. Cosmochim. Acta* **67**, 641–653.
- Alt J. C., Shanks, III, W. C., Bach W., Paulick H., Garrido C. J. and Baudoin G. (2007) Hydrothermal alteration and microbial sulfate reduction in peridotite and gabbro exposed by detachment faulting at the Mid-Atlantic Ridge, 15°N20°N (ODP Leg 209): a sulfur and oxygen isotope study. *Geochem. Geophys. Geosyst.* **8**. doi:10.1029/2007GC001617.
- Bach W., Banerjee N. R., Dick H. J. B. and Baker E. T. (2002) Discovery of ancient and active hydrothermal deposits along the ultraslow spreading Southwest Indian Ridge 10–16°E. *Geochem. Geophys. Geosyst.* **3**. doi:10.1029/2001GC000279.
- Bach W., Garrido C. J., Harvey J., Paulick H. and Rosner M. (2004) Variable seawater–peridotite interactions—first insights from ODP Leg 209, MAR 15°N. *Geochem. Geophys. Geosyst.* **5**. doi:10.1029/2004GC000744.
- Bach W., Paulick H., Garrido C. J. and Ildefonse B. (2006) Unraveling the sequence of serpentinization reactions: petrography, mineral chemistry, and petrophysics of serpentinites from MAR 15°N (ODP Leg 209, Site 1274). *Geophys. Res. Lett.* **5**. doi:10.1029/2006GL025681.
- Baes C. F. and Mesmer R. E. (1976) *The Hydrolysis of Cations*. Wiley, New York.
- Barnes I. and O'Neil J. R. (1969) The relationship between fluids in some fresh alpine-type ultramafics and possible modern serpentinization, western United States. *Geol. Soc. Am. Bull.* **80**, 1947–1960.
- Berndt M. E., Allen D. E. and Seyfried, Jr., W. E. (1996) Reduction of CO₂ during serpentinization of olivine at 300 °C and 500 bar. *Geology* **24**, 351–354.
- Boschi C., Früh-Green G. L. and Delacour A. (2006) Mass transfer and fluid flow during detachment faulting and development of an oceanic core complex, Atlantis Massif (MAR 30°N). *Geochem. Geophys. Geosyst.* **7**. doi:10.1029/2005GC001074.
- Brazelton W. J., Schrenk M. O., Kelley D. S. and Baross J. A. (2006) Methane- and sulfur-metabolizing microbial communities dominate the Lost City Hydrothermal Field ecosystem. *Appl. Environ. Microbiol.* **72**, 6257–6270.
- Chapelle F. H., O'Neill K., Bradley P. M., Methe B. A., Ciuffo S. A., Knobel L. L. and Lovley D. R. (2002) A hydrogen-based subsurface microbial community dominated by methanogens. *Nature* **415**, 312–315.
- Charlou J.-L. and Donval J. P. (1993) Hydrothermal methane venting between 12°N and 26°N along the Mid-Atlantic Ridge. *J. Geophys. Res.* **98**, 9625–9642.
- Charlou J.-L., Fouquet Y., Bougault H., Donval J. P., Etoubleau J., Jean-Baptiste P., Dapoigny A., Appriou P. and Rona P. A. (1998) Intense CH₄ plumes generated by serpentinization of ultramafic rocks at the intersection of the 15°20'N fracture zone and the Mid-Atlantic Ridge. *Geochim. Cosmochim. Acta* **62**, 2323–2333.
- Charlou J.-L., Donval J. P., Fouquet Y., Jean-Baptiste P. and Holm N. (2002) Geochemistry of high H₂ and CH₄ vent fluids issuing from ultramafic rocks at the Rainbow hydrothermal field (36°14'N, MAR). *Chem. Geol.* **191**, 345–359.
- Coleman R. G. (1967) Low-temperature reaction zones and alpine ultramafic rocks of California, Oregon, and Washington. *US Geol. Survey Bull.* **1247**, 1–49.
- D'Antonio M. and Kristensen M. B. (2004) Serpentine and brucite of ultramafic clasts from the South Chamorro Seamount (Ocean Drilling Program Leg 195, Site 1200): inferences for the serpentinization of the Mariana forearc mantle. *Mineral. Mag.* **68**, 887–904.
- Dyment J., Arkani-Hamed J. and Ghods A. (1997) Contribution of serpentinized ultramafics to marine magnetic anomalies at slow and intermediate spreading centers: insights from the shape of the anomalies. *Geophys. J. Int.* **129**, 691–701.
- Evans B. W. and Trommsdorf V. (1970) Regional metamorphism of ultramafic rocks in the Central Alps. Paragenesis in the system CaO–MgO–SiO₂–H₂O. *Schweiz. Min. Pet. Mitt.* **50**, 481–492.
- Evans B. W. and Trommsdorf V. (1972) Die einfluss des eisens auf die hydratisierung von duniten. *Schweiz. Min. Pet. Mitt.* **52**, 251–256.
- Fisk M. R. and Giovannoni S. J. (1999) Sources of nutrients and energy for a deep biosphere on Mars. *J. Geophys. Res.* **104**, 11805–11815.
- Foustoukos D. I. and Seyfried, Jr., W. E. (2004) Hydrocarbons in hydrothermal vent fluids: the role of chromium-bearing catalysts. *Science* **304**, 1002–1005.
- Frost B. R. (1985) On the stability of sulfides, oxides, and native metals in serpentinite. *J. Petrol.* **26**, 31–63.
- Frost B. R. and Beard J. S. (2007) On silica activity and serpentinization. *J. Petrol.* **48**, 1351–1368.
- Früh-Green G. L., Plas A. and Lécuyer C. (1996) Petrologic and stable isotope constraints on hydrothermal alteration and serpentinization of the EPR shallow mantle at Hess Deep (Site 895). *Proc. ODP Sci. Res.* **147**, 255–290.
- Früh-Green G. L., Connolly J. A. D., Plas A., Kelley D. S. and Grobéty B. (2004) Serpentinization of ocean peridotites: implications for geochemical cycles and biological activity. In *The Seafloor Biosphere at Mid-Ocean Ridges* (eds. W. S. D. Wilcock, E. F. DeLong, D. S. Kelley, J. A. Baross and S. C.

- Cary). American Geophysical Union, Washington, DC, pp. 119–136.
- Fu Q., Sherwood Lollar B., Horita J., Lacrampe-Couloume G. and Seyfried, Jr., W. E. (2007) Abiotic formation of hydrocarbons under hydrothermal conditions: constraints from chemical and isotope data. *Geochim. Cosmochim. Acta* **71**, 1982–1998.
- Gold T. J. (1979) Terrestrial sources of carbon and earthquake outgassing. *J. Petrol. Geol.* **1**, 3–19.
- Gold T. J. (1999) *The Deep Hot Biosphere*. Copernicus, New York.
- Helgeson H. C., Delany J. M., Nesbitt H. W. and Bird D. K. (1978) Summary and critique of the thermodynamic properties of rock-forming minerals. *Am. J. Sci.* **278-A**, 1–229.
- Helgeson H. C., Kirkham D. H. and Flowers G. C. (1981) Theoretical prediction of the thermodynamic behavior of aqueous electrolytes at high pressures and temperatures: IV. Calculation of activity coefficients, osmotic coefficients, and apparent molal and standard and relative partial molal properties to 600 °C and 5 Kb. *Am. J. Sci.* **281**, 1249–1516.
- Holm N. G. and Andersson E. M. (1998) Hydrothermal systems. In *The Molecular Origins of Life* (ed. A. Brack). Cambridge University Press, pp. 86–99.
- Holm N. G. and Charlou J.-L. (2001) Initial indications of abiotic formation of hydrocarbons in the Rainbow ultramafic hydrothermal system, Mid-Atlantic Ridge. *Earth Planet. Sci. Lett.* **191**, 1–8.
- Horita J. and Berndt M. E. (1999) Abiogenic methane formation and isotopic fractionation under hydrothermal conditions. *Science* **285**, 1055–1057.
- Hostetler P. B., Coleman R. G. and Evans B. W. (1966) Brucite in alpine serpentinites. *Am. Mineral.* **51**, 75–98.
- Johnson J. W., Oelkers E. H. and Helgeson H. C. (1992) SUPCRT92: a software package for calculating the standard molal thermodynamic properties of minerals, gases, aqueous species, and reactions from 1 to 5000 bar and 0 to 1000 °C. *Comput. Geosci.* **18**, 899–947.
- Johnson O. J., Morrill P., Muyzer G., Kuenen J. G. and Neelson K. H. (2006) Ultrabasic spring geomicrobiology of the Cedars Peridotite. *Eos Trans. AGU* 87(52), Fall Meet. Suppl., Abstract B12B-05.
- Kelley D. S. and Früh-Green G. L. (1999) Abiogenic methane in deep-seated mid-ocean ridge environments: insights from stable isotope analyses. *J. Geophys. Res.* **104**, 10439–10460.
- Kelley D. S., Karston J. A. and Blackman D. K., et al. (2001) An off-axis hydrothermal vent field near the Mid-Atlantic Ridge at 30°N. *Nature* **412**, 145–149.
- Kelley D. S., Karston J. A., Früh-Green G. L., Yoerger D. R., Shank T. M., Butterfield D. A., Hayes J. M., Schrenk M. O., Olson E. J., Proskurowski G., Jakuba M., Bradley A., Larson B., Ludwig K., Glickson D., Buckman K., Bradley A. S., Brazelton W. J., Roe K., Elend M. J., Delacour A., Bernasconi S. M., Lilley M. D., Baross J. A., Summons R. E. and Sylva S. P. (2005) A serpentinite-hosted ecosystem: the Lost City hydrothermal field. *Science* **307**, 1428–1434.
- Kozlov I. T. and Levshov P. P. (1962) Amakinite, a new mineral of the brucite-pyrrhoite group. *Am. Mineral.* **47**, 1218 (translation from Russian).
- Martin W. and Russell M. J. (2006) On the origin of biochemistry at an alkaline hydrothermal vent. *Phil. Trans. R. Soc. Lond. B* **362**, 1887–1925.
- McCollom T. M. (1999) Methanogenesis as a potential source of chemical energy for primary biomass production by autotrophic organisms in hydrothermal systems on Europa. *J. Geophys. Res.* **104**, 30729–30742.
- McCollom T. M. (2007) Geochemical constraints on sources of metabolic energy for chemolithoautotrophy in ultramafic-hosted deep-sea hydrothermal systems. *Astrobiology* **7**, 933–950.
- McCollom T. M. and Seewald J. S. (2001) A reassessment of the potential for reduction of dissolved CO₂ to hydrocarbons during serpentinization of olivine. *Geochim. Cosmochim. Acta* **65**, 3769–3778.
- McCollom T. M. and Seewald J. S. (2003) Experimental constraints on the hydrothermal reactivity of organic acids and acid anions: I. Formic acid and formate. *Geochim. Cosmochim. Acta* **67**, 3625–3644.
- McCollom T. M. and Seewald J. S. (2007) Abiotic synthesis of organic compounds in deep-sea hydrothermal environments. *Chem. Rev.* **107**, 382–401.
- McCollom T. M. and Shock E. L. (1998) Fluid–rock interactions in the lower oceanic crust: thermodynamic models of hydrothermal alteration. *J. Geophys. Res.* **103**, 547–576.
- Mével C. (2003) Serpentinization of abyssal peridotites at mid-ocean ridges. *C. R. Geosci.* **335**, 825–852.
- Mével C. and Stamoudi C. (1996) Hydrothermal alteration of the upper-mantle section at Hess Deep. *Proc. ODP Sci. Res.* **147**, 293–309.
- Miroshnichenko M. L., L'Haridon S., Nercessian O., Antipov A. N., Kostrikina N. A., Tindall B. J., Schumann P., Spring S., Stackebrandt E., Bonch-Osmolovskaya E. A. and Jeanthon C. (2003a) *Vulcanithermus mediatlanticus* gen. Nov., sp. nov., a novel member of the family *Thermaceae* from a deep-sea hot vent. *Int. J. Syst. Evol. Microbiol.* **53**, 1143–1148.
- Miroshnichenko M. L., Slobodkin A. I., Kostrikina N. A., L'Haridon S., Nercessian O., Spring S., Stackebrandt E., Bonch-Osmolovskaya E. A. and Jeanthon C. (2003b) *Deferritibacter abyssi* sp. Nov., an anaerobic thermophile from deep-sea hydrothermal vents of the Mid-Atlantic Ridge. *Int. J. Syst. Evol. Microbiol.* **53**, 1637–1641.
- Moody J. B. (1976a) Serpentinization: a review. *Lithos* **9**, 125–138.
- Moody J. B. (1976b) An experimental study on the serpentinization of iron-bearing olivines. *Can. Mineral.* **14**, 462–478.
- Neal C. and Stanger G. (1983) Hydrogen generation from mantle source rocks in Oman. *Earth Planet. Sci. Lett.* **66**, 315–320.
- Neelson K. H., Inagaki F. and Takai K. (2005) Hydrogen-driven subsurface lithoautotrophic microbial ecosystems (SLiMEs): do they exist and why should we care? *Trends Microbiol.* **13**, 405–410.
- O'Hanley D. S. (1996) *Serpentinites: Records of Tectonic and Petrological History*. Oxford University Press, New York.
- Oufi O., Cannat M. and Horen H. (2002) Magnetic properties of variably serpentinized abyssal peridotite. *J. Geophys. Res.* **107**. doi:10.1029/2001JB000549.
- Page N. J. (1967) Serpentinization at Burro Mountain, Calif. *Contr. Mineral. Petrol.* **14**, 321–342.
- Palandri J. L. and Reed M. H. (2004) Geochemical models of metasomatism in ultramafic systems: serpentinization, rodingitization, and sea floor carbonate chimney precipitation. *Geochim. Cosmochim. Acta* **68**, 1115–1133.
- Proskurowski G., Lilley M. D., Kelley D. S. and Olson E. J. (2006) Low temperature volatile production at the Lost City Hydrothermal Field, evidence from a hydrogen stable isotope geothermometer. *Chem. Geol.* **229**, 331–343.
- Proskurowski G., Lilley M. D., Seewald J. S., Früh-Green G. L., Olson E. J., Lupton J. E., Sylva S. P. and Kelley D. S. (2008) Abiogenic hydrocarbon production at Lost City Hydrothermal Field. *Science* **319**, 604–607.
- Réfait Ph., Bon C., Simon L., Bourrié Trolard F., Bessière J. and Génin J.-M. R. (1999) Chemical composition and Gibbs standard free energy of formation of Fe(II)–Fe(III) hydroxysulfate green rust and Fe(II) hydroxide. *Clay Miner.* **34**, 499–510.

- Russell M. J. (2007) The alkaline solution to the emergence of life: energy, entropy, and early evolution. *Acta Biotheoret.* **55**, 133–179.
- Sassani, D. C. (1992) Petrologic and thermodynamic investigation of the aqueous transport of platinum-group elements during alteration of mafic intrusive rocks. Ph.D. thesis, Washington University at St. Louis.
- Schrenk M. O., Kelley D. S., Baross J. A. and Delaney J. R. (2004) Low archaeal diversity linked to seafloor geochemical processes at the lost City Hydrothermal Field, Mid-Atlantic Ridge. *Environ. Microbiol.* **6**, 1086–1095.
- Schulte M., Blake D., Hoehler T. and McCollom T. M. (2006) Serpentinization and its implications for life on the early Earth and Mars. *Astrobiology* **6**, 364–376.
- Seewald J. S., Zolotov M. Yu. and McCollom T. M. (2006) Experimental investigation of single carbon compounds under hydrothermal conditions. *Geochim. Cosmochim. Acta* **70**, 446–460.
- Seward T. M. and Franck E. U. (1981) The system hydrogen–water up to 440 °C and 2500 bar pressure. *Ber. Bunsenges. Phys. Chem.* **85**, 2–7.
- Seyfried, Jr., W. E., Foustoukos D. I. and Fu Q. (2007) Redox evolution and mass transfer during serpentinization: an experimental and theoretical study at 200 °C, 500 bar with implications for ultramafic-hosted hydrothermal systems at Mid-Ocean Ridges. *Geochim. Cosmochim. Acta* **71**, 3872–3886.
- Shock E. L. and Helgeson H. C. (1988) Calculation of the thermodynamic and transport properties of aqueous species at high pressure and temperatures: correlation algorithms for ionic species and equation of state predictions to 5 kb and 1000 °C. *Geochim. Cosmochim. Acta* **52**, 2009–2036.
- Shock E. L. and Schulte M. D. (1998) Organic synthesis during fluid mixing in hydrothermal systems. *J. Geophys. Res.* **103**, 28513–28517.
- Shock E. L., Helgeson H. C. and Sverjensky D. A. (1989) Calculation of the thermodynamic and transport properties of aqueous species at high pressures and temperatures: standard partial molal properties of inorganic neutral species. *Geochim. Cosmochim. Acta* **53**, 2157–2183.
- Shock E. L., Sassani D. C., Willis M. and Sverjensky D. A. (1997) Inorganic species in geologic fluids: correlations among standard molal thermodynamic properties of aqueous ions and hydroxide complexes. *Geochim. Cosmochim. Acta* **61**, 907–950.
- Sleep N. H., Meibom A., Fridriksson Th., Coleman R. G. and Bird D. K. (2004) H₂-rich fluids from serpentinization: geochemical and biotic implications. *Proc. Natl. Acad. Sci. USA* **101**, 12818–12823.
- Sverjensky D. A. (1992) Linear free energy relations for predicting dissolution rates of solids. *Nature* **358**, 310–313.
- Sverjensky D. A. and Molling P. A. (1992) A linear free energy relationship for crystalline solids and aqueous ions. *Nature* **356**, 231–234.
- Szatmari P. (1989) Petroleum formation by Fischer–Tropsch synthesis in plate tectonics. *Am. Assoc. Petrol. Geol. Bull.* **73**, 989–998.
- Takai K., Gamo T., Tsunogai U., Nakayama H., Nealson K. H. and Horikoshi K. (2004) Geochemical and microbiological evidence for a hydrogen-based, hyperthermophilic subsurface lithoautotrophic microbial ecosystem (HyperSLiME) beneath an active deep-sea hydrothermal field. *Extremophiles* **8**, 269–282.
- Takai K., Nakamura K., Suzuki K., Inagaki F., Nealson K. H. and Kumagai H. (2006) Ultramafics-Hydrothermalism-Hydrogenesis-HyperSLiME (UltraH³) linkage: a key insight into early microbial ecosystem in the Archean deep-sea hydrothermal systems. *Paleont. Res.* **10**, 269–282.
- Toft P. B., Arkani-Hamed J. and Haggerty S. E. (1990) The effects of serpentinization on density and magnetic susceptibility: a petrophysical model. *Phys. Earth Planet. Int.* **65**, 137–157.
- Von Damm K. L. (1995) Controls on the chemistry and temporal variability of seafloor hydrothermal fluids. In *Seafloor Hydrothermal Systems: Physical, Chemical, Biological, and Geological Interactions* (eds. S. E. Humphris, R. A. Zierenberg, L. S. Mullineaux and R. E. Thomson). American Geophysical Union, DC, Washington, pp. 222–247.
- Voordeckers J. W., Starovoytov V. and Vetricani C. (2005) *Caminibacter medianticus* sp. Nov., a thermophilic, chemolithoautotrophic nitrate-ammonifying bacterium isolated from a deep-sea hydrothermal vent on the Mid-Atlantic Ridge. *Int. J. Syst. Evol. Microbiol.* **55**, 773–779.
- Wagman D. D., Evans W. H., Parker V. B., Schumm R. H., Halow I., Bailey S. M., Churney K. L. and Nuttall R. L. (1982) The NBS tables of chemical thermodynamic properties. Selected values for inorganic and C₁ and C₂ organic substances in SI units. *J. Phys. Chem. Ref. Data* **11**(suppl. 2), 1–392.
- Wegner W. W. and Ernst W. G. (1983) Experimentally determined hydration and dehydration reaction rates in the system MgO–SiO₂–H₂O. *Am. J. Science* **283-A**, 151–180.
- Wetzel L. R. and Shock E. L. (2000) Distinguishing ultramafic-hosted from basalt-hosted submarine hydrothermal systems by comparing calculated vent fluid compositions. *J. Geophys. Res.* **105**, 8319–8340.
- Wolery T. J. (1992) *EQ3/6, A Software Package for Geochemical Modeling of Aqueous Systems: Package Overview and Installation Guide (Version 7.0)*. Lawrence Livermore National Laboratory, Livermore, CA.
- Wolery T. J. and Daveler S. A. (1992) *EQ6, A Computer Program for Reaction Path Modeling of Aqueous Geochemical Systems: Theoretical Manual, User's Guide, and Related Documentation (Version 7.0)*. Lawrence Livermore National Laboratory, Livermore, CA.